

Materials Advances

Accepted Manuscript

This article can be cited before page numbers have been issued, to do this please use: M. Segale, T. Seadira, R. Sigwadi, T. Mokrani and G. Summers, *Mater. Adv.*, 2024, DOI: 10.1039/D4MA00628C.



This is an Accepted Manuscript, which has been through the Royal Society of Chemistry peer review process and has been accepted for publication.

Accepted Manuscripts are published online shortly after acceptance, before technical editing, formatting and proof reading. Using this free service, authors can make their results available to the community, in citable form, before we publish the edited article. We will replace this Accepted Manuscript with the edited and formatted Advance Article as soon as it is available.

You can find more information about Accepted Manuscripts in the [Information for Authors](#).

Please note that technical editing may introduce minor changes to the text and/or graphics, which may alter content. The journal's standard [Terms & Conditions](#) and the [Ethical guidelines](#) still apply. In no event shall the Royal Society of Chemistry be held responsible for any errors or omissions in this Accepted Manuscript or any consequences arising from the use of any information it contains.

1 A New Frontier Towards Development of Efficient SPEEK Polymer 2 Membranes for PEM Fuel Cells Applications: A Review

3 Mayetu Segale^a, Tumelo Seadira^{a*}, Rudzani Sigwadi^a, Touhami Mokrani^a, Gabriel Summers^b,

4 ^aDepartment of Chemical and Materials Engineering (CSET), University of South Africa (Science Campus), Private
5 Bag X6, Florida Park, Roodepoort, 1709, South Africa.

6 ^bDepartment of Chemistry (CSET), University of South Africa (Science Campus), Private Bag X6, Florida Park,
7 Roodepoort, 1709, South Africa.

8

9 Abstract

10 Proton exchange membrane fuel cells (PEMFCs) have gained popularity over the last decade as a
11 potential clean energy source for electric vehicles and portable electronic devices. Nafion is commonly
12 used as a membrane material but suffers from high methanol crossover and cost. These drawbacks
13 negatively influence the widespread commercial application of PEMFCs. Currently, the focus is on
14 developing high-performance, low-cost PEMs to replace Nafion membranes. Sulfonated poly-ether-
15 ketone-ether (SPEEK) has been identified as a promising alternative PEM in fuel cell applications due
16 to its advantageous properties, such as low cost, mechanical and chemical stability, and ease of
17 preparation and operation. The main purpose of this review is to demonstrate the benefits of SPEEK-
18 based composite membranes over Nafion® by mixing the SPEEK material with fluorinated polymers,
19 hydrocarbon polymers, carbon-based materials, metal oxide materials, etc. The ion-exchange capacity
20 and proton conductivity of SPEEK polymer with different fillers are highlighted. SPEEK-based
21 composite membranes are far more suitable for PEMFC and DMFC applications because SPEEK
22 polymer is produced in an environmentally friendly manner. This critical review guides researchers in
23 developing processes to maximise the SPEEK-based membrane's properties for fuel cell applications.

24 Keywords: Polymers, Composite membranes, SPEEK-based membranes, PEM Fuel Cells

25

26 1. Introduction

27 For decades, fossil fuels have been considered the main sources of the increased
28 pollution levels in the environment due to the emission of toxic greenhouse gases
29 such as CO_x, NO_x, and SO_x upon their combustion [1-3]. Furthermore, there are
30 growing concerns about the long-term viability of fossil fuels which are expected to
31 run out sooner rather than later. As a result, sustainable, renewable, and
32 environmentally friendly fuels will emerge sooner or later.

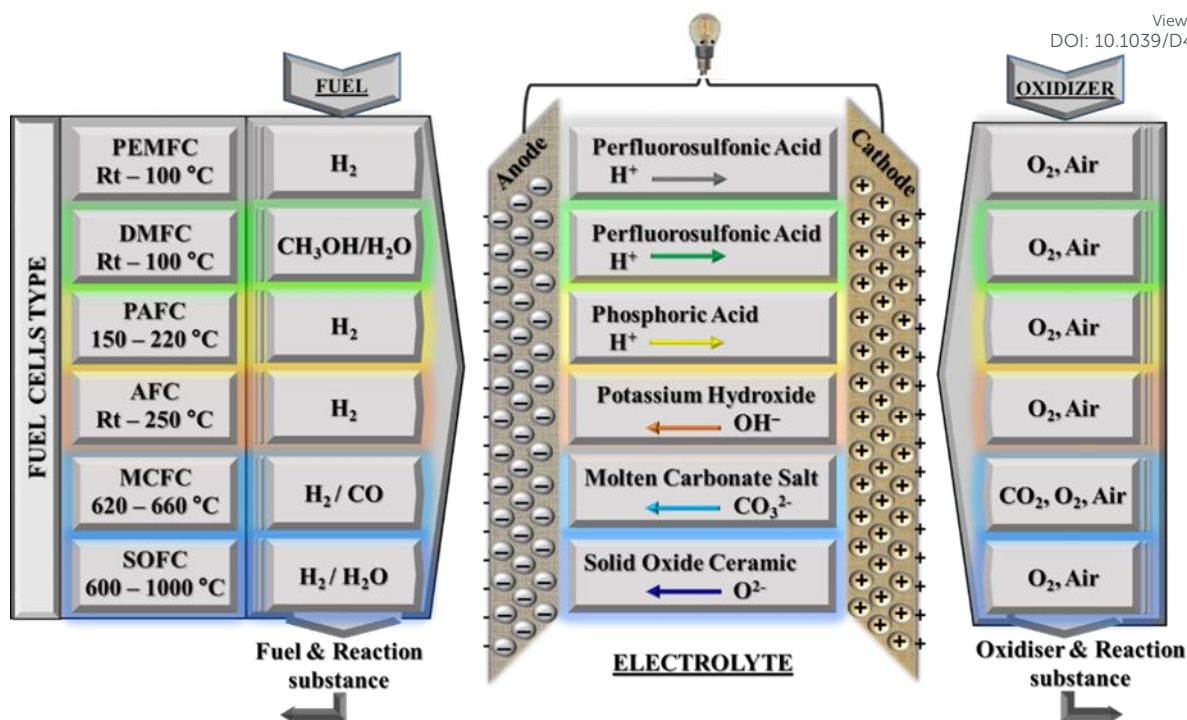
33 * Corresponding Author: Tumelo Seadira (tumelo.seadira@gmail.com)



34 To address these issues, extensive research and development are being conducted
35 to identify alternative sources of electricity that are efficient, renewable, and
36 environmentally friendly. Fuel cells are one of many technologies that will enable future
37 sustainable hydrogen, carbon-free cycles, and a circular economy [4, 5]. Over the last
38 two decades, fuel cell applications have grown in popularity as engines, stationary and
39 portable power sources. [6, 7]. Mohammed et al.,[8] described a fuel cell as an
40 electrochemical device that converts chemical energy of a fuel (the reactant) such as
41 methanol, ethanol or ethylene glycol into electrical energy without any fuel combustion.
42 The fuel is directly oxidised, producing electricity, heat, and water vapour. The
43 electrochemical reactions within the fuel cell are explained as follows: When hydrogen
44 passes through the anode, it is converted into hydrogen ions, and electrons are
45 released, which travel through an external circuit before reaching the cathode to
46 produce electrical current. [9]. The membrane electrode assembly (MEA) is the
47 primary component of the fuel cell, consisting of a gas diffusion layer, catalyst, and
48 electrolyte (membrane). The protons migrate through the electrolyte to the cathode,
49 where they unite with oxygen and the electrons to produce water and heat. Fuel cell
50 technologies are characterized by the nature of electrolyte they use. The electrolyte is
51 one of the important part of the fuel cells as it defines the properties and the operating
52 conditions of the fuel cell [10, 11]. There are six distinct types of fuel cells namely, (i)
53 Alkaline Fuel Cell (AFC), (ii) Direct Methanol Fuel Cell (DMFC), (iii) Molten Carbonate
54 Fuel Cell (MCFC), (iv) Phosphoric Acid Fuel Cell (PAFC), (v) Proton Exchange
55 Membrane Fuel Cell (PEMFC) and (vi) Solid Oxide Fuel Cell (SOFC), each operating
56 at different reaction conditions and use different electrolytes. Out of the six fuel cells,
57 two fuel cells (i.e. hydrogen Fuel Cell (H₂-FC) and direct methanol fuel cell (DMFC))
58 use polymeric membrane as an electrolyte, while others are based on the
59 electrochemical principles. The components, fuel types and performance
60 characteristics of the types various of Fuel Cells are presented in Figure 1.

View Article Online
DOI: 10.1059/D4MA00628C



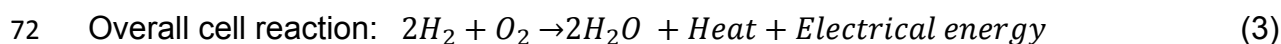
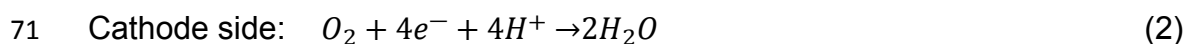
View Article Online
DOI: 10.1039/D4MA00628C

61

62 Figure 1. Schematic representation of different types of Fuel Cells and their properties

63

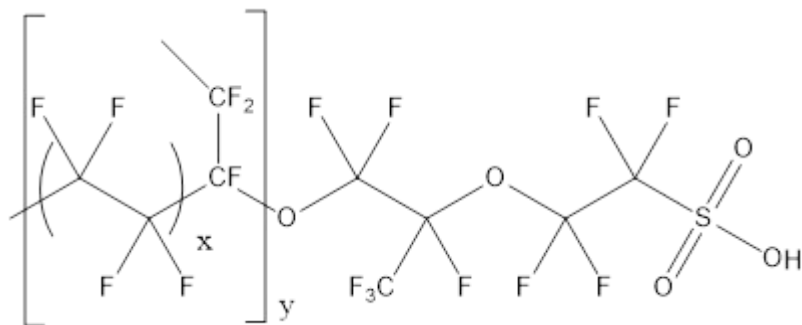
64 Among the fuel cells listed above, proton exchange membrane fuel cell (PEMFC)
 65 technology is a major area of global research interest [12]. Their high energy density
 66 and efficiency, along with their potential for low emissions, make them a promising
 67 clean energy technology. The proton exchange membrane (PEM) acts as a barrier to
 68 the fuel gas between the electrodes, transferring protons from the anode to the
 69 cathode of the PEMFC. The reactions that occur in the PEMFC are as follows.



73 For the anodic reaction, hydrogen flows through the gas diffusion layer before
 74 dissociating into two electrons and two protons in the catalyst layer (equation 1). The
 75 two protons pass through the PEM to reach the catalyst layer at the cathode, and the
 76 two electrons pass through the external circuit to the cathode [13, 14]. Similar to the
 77 anodic reaction, which results in the production of heat and water, the cathodic
 78 reaction occurs when air enters the catalyst layer through the gas diffusion layer and



79 reacts with the two electrons and two protons (equation 2). The most common
80 membranes used in PEM fuel cells are fluorinated membranes. The perfluorosulfonic
81 acid (PFSA) polymers known as Nafion membranes are the most common type.
82 Sulfonated polymers, such as Nafion, with perfluorinated backbones and sulfonated
83 side-chains, are the most widely used membrane for PEM cells because they function
84 well at temperatures below 100 °C. Perfluoroether in Nafion is responsible for chemical
85 stability, while sulfonated sidechains aggregate and facilitate hydration [15]. Due to its
86 high ionic conductivity (approximately 0.1 S/cm when fully hydrated), as well as its
87 thermal and chemical stability, Nafion membrane has been chosen as a standard for
88 polymeric electrolyte fuel cells [16]. However, Nafion membranes have several
89 drawbacks, including a decrease in ionic conductivity and low humidity at high
90 temperatures, which makes commercialization difficult. For these reasons, other
91 proton conducting membranes with either partially fluorinated or hydrocarbon-based
92 polymers containing ionic transfer sites have been developed to improve fuel cell
93 performance. The chemical structure of Nafion is shown in Figure 2.



95
96 Figure 2. Chemical structure of Nafion.

97
98 In this context, many studies have been conducted to develop PEM with improved
99 performance characteristics such as low cost, ease of synthesis, good thermal and
100 mechanical stability, and eco-friendliness. Partially fluorinated PEM can be created by
101 synthesizing block copolymers, one of which is a fluoropolymer. Partially fluorinated
102 membranes, like fluorinated membranes, have demonstrated high proton conductivity.
103 However, it is costly and cannot be referred to as low cost due to the use of expensive

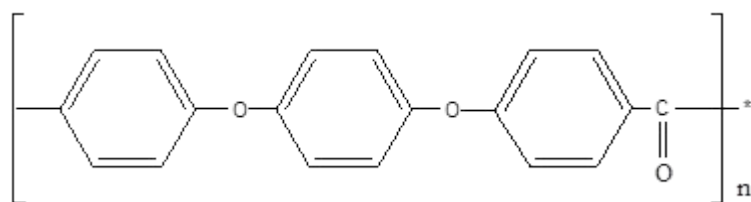


104 fluorinated materials. Furthermore, commercialization of these materials has been
105 hampered by high costs and a scarcity of trifluorostyrene monomer [16].

106 Non-fluorinated membranes are made from polymer materials with aromatic structures
107 and functional groups in either the polymeric backbone or side groups are being used
108 in the proton exchange membranes (PEMs) in place of perfluorinated membranes.

109 One major advantage of hydrocarbon membranes is that it's simple to design the
110 polymeric structure to have the right characteristics for fuel cell applications [17].
111 Various types of monomers are used to control the reaction conditions when preparing
112 hydrocarbon membranes with excellent properties. Moreover, the cost of the
113 monomers used in the production of hydrocarbon-based polymers is comparatively
114 lower than that of fluorinated membranes, which is a major benefit for
115 commercialization [15, 18]. In general, hydrocarbon-based polymers have polar
116 groups and a carbon backbone, and they have high water uptake over a wide
117 temperature range. Despite having increased proton conductivity and poor
118 dimensional stability in membranes, water channel formation occurs [19]. Rigid sites,
119 such as aromatic structures, are incorporated directly into the polymer backbone to
120 improve membrane stability and properties. The aromatic rings provide rigidity, which
121 leads to thermal and mechanical stability. As a result, a variety of hydrocarbon-based
122 polymers, including, poly-ether ketones (PEK), poly(arylene ethers), polyether ether
123 ketone (PEEK), polyesters, and polyimides (PI), have been actively researched and
124 developed for use in fuel cell applications [20-23]. With a wide variety of alternative
125 aromatic polymers to choose from, polyether ether ketone (PEEK) appears to have
126 the best potential as a PEM for fuel cell application. PEEKs are semicrystalline
127 thermoplastic polymers with ether and ketone chemical properties. This polymer has
128 a well-balanced blend of excellent mechanical properties, low cost and superior
129 thermo-oxidative stability [22]. PEEK polymer has an aromatic, nonfluorinated
130 backbone with 1,4-disubstituted phenyl groups separated by ether (—O—) and
131 carbonyl (—C=O) linkages (as shown on Figure 3 below), making it a high-
132 performance thermostable engineering polymer [24].





View Article Online
DOI: 10.1039/D4MA00628C

133

134 Figure 3. General structure of PEEK [24].

135

136 This polymer's inherent hydrophobicity is typically overcome through chemical
137 modification of the polymer chains. Sulfonic acid functionalities are easily incorporated
138 onto the aromatic backbone of PEEK. Sulfonated poly(ether ether ketone) (SPEEK) is
139 a semi-crystalline, amorphous polymer that exhibits high chemical and thermal
140 stabilities due to the presence of aromatic rings [25]. It is made by polymerizing
141 different monomers using the following synthesis techniques: (i) displacement
142 reaction; (ii) nickel-catalyzed coupling polymerization; (iv) ring-opening polymerization
143 involving monomers with sulfonic acid groups; and (iii) Friedel-Craft acylation [26]. The
144 degree of sulfonation (DS) has a strong influence on the properties of SPEEK, which
145 can be controlled by adjusting the reaction conditions (reaction temperature, acid
146 concentration, and sulfonation time). The SPEEK demonstrated desirable chemical
147 durability at low DS, with greater dimensional, mechanical, and thermal stability than
148 Nafion but lower water uptake and proton conductivity [27]. At higher DS, membrane
149 swelling in aqueous solutions promotes the formation of interconnected channels of
150 hydrophilic clusters. This resulted in high proton conductivity similar to Nafion, but with
151 undesirable mechanical properties, excessive dimensional swelling, fuel permeability,
152 and consequently low durability. Many studies have been conducted to develop
153 modified SPEEK membranes in order to improve fuel cell performance [28, 29].

154 The intensive research activities in the development of modified SPEEK membranes,
155 particularly for fuel cell applications, are critical for evaluating progress in this specific
156 research field. With considerable efforts made to enhance SPEEK membranes, this
157 review concentrates on the development of PEMs based on sulfonated poly(ether
158 ether ketone) (SPEEK) polymers. The physicochemical properties and characteristics
159 of pure sulfonated polyether ether ketone membranes (SPEEK) are discussed. The
160 article also discusses strategies for improving the performance of the SPEEK matrix
161 membrane. The results for various types of modified SPEEK membranes are



162 summarised and analysed. This paper concludes with the challenges and
 163 opportunities encountered during the development of SPEEK-based membranes for
 164 fuel cell applications.

165

166 2. Mechanism of proton conduction in PEM

167 Proton conduction is the most important factor to consider when assessing
 168 membranes for possible fuel cell applications. In PEMFC operation, the membrane
 169 must ensure the systematic movement of water and ions, rejection of electrons, and
 170 dissociation of reactant gases. Sufficient hydration levels of PEM are critical for
 171 maintaining high proton conductivity during fuel cell operation. Two major mechanisms
 172 can hydrate proton transfer at the molecular level: electro-osmotic drag (vehicle) and
 173 proton hopping (Grotthuss) [30]. A schematic design of the Grotthuss and vehicular
 174 mechanisms is shown in Figure 4.

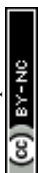


175

176 Figure 4. A schematic representation of the Grotthuss and vehicular mechanisms [31].

177

178 In the proton hopping (Grotthuss) mechanism, protons move from one hydrolyzed ion
 179 (SO_3^- , H_3O^+) to another via polymeric matrices. The activation energy required for
 180 proton conductivity to occur for this proton hopping mechanism is 0.1- 0.4 eV. Protons
 181 are drawn from the hydronium ions by more adjacent water molecules, and the cycle
 182 is repeated. In this mechanism, the ion area forms a specific hydrophilic cluster that
 183 expands with water. As a result, protons will undergo percolation mechanisms. The



184 Grotthus mechanism contributes to the conductivity of a perfluorinated sulfonic acid
185 membrane like Nafion [32].

186 The ion exchange capacity (IEC) value affects Grotthus-type transfer because it
187 represents the number of ionizable groups loaded into the fuel cell membrane. Electro-
188 osmotic drag (vehicle) in the membrane transports hydrogen ions (H_3O^+) throughout
189 the aqueous medium. As a result, water and methanol molecules act as proton
190 transporters in the polymeric membrane. The activation energy is required to initiate
191 proton conductivity $E_{act} > 0.5$ eV [33]. In this mechanism, hydrated protons
192 (hydronium ions) permeate an aqueous medium due to electrochemical differences.
193 Protons bind to vehicles such as water or methanol before diffusing into the medium
194 to form cationic complexes such as H_3O^+ , $H_5O_2^+$, $H_9O_4^+$, and $CH_3OH_2^+$. The presence
195 of free volumes in the polymeric chain of proton exchange membranes is critical to the
196 vehicular mechanism. Water aids proton conductivity in PEM by influencing size,
197 stability, production, clusters and ion route connection. In aqueous conditions, as
198 cluster size increases, proton conductivity increases in proportion to humidity. The
199 proton conductivity of polymeric membranes at high temperatures and low relative
200 humidity could be enhanced by choosing inorganic additives using this mechanism
201 [34].

202 3. Sulfonation of PEEK

203 Poly (ether ether ketone) polymers are chemically resistant, thermally and
204 mechanically stable. However, due to their completely hydrophobic segments, they
205 cannot be used directly in fuel cell applications [29]. As a result, adding a sulfonic acid
206 group to PEEK polymer improves its hydrophilicity, solubility in polar solvents, and ion
207 exchange capacity. At different degrees of sulfonation, the sulfonated form (SPEEK)
208 is soluble in different solvents. The solubility of the SPEEK membrane is reported as
209 follows: A sulfonation degree (DS) of about 30% makes it soluble only in hot DMF,
210 DMAc, DMSO, and NMP; a DS of 40–70% makes it soluble at room temperature in
211 DMF, DMAc, DMSO, and NMP; a DS of above 70% makes it soluble in methanol; and
212 a DS of 100% makes it soluble in hot water [35]. Three synthetic methods can be used
213 to prepare sulfonated poly(ether ether ketone):

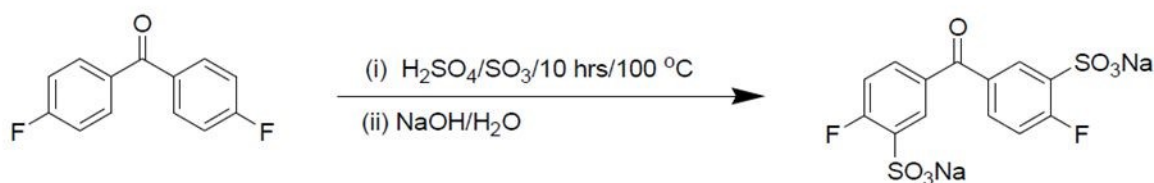
- 214 (a) Direct sulfonated monomer copolymerization reactions with suitable monomers.
- 215 (b) Direct post-polymerization sulfonation reactions with poly(ether ether ketone).



216 (c) Sulfonation reactions of poly(ether ether ketone)s to introduce the sulfonate group
 217 pendant into the polymer chains.

218 3.1 Direct sulfonated monomer copolymerization reactions with suitable 219 monomers.

220 A specific sulfonated dihalogenated diaryl ketone monomer or sulfonated bisphenol
 221 derivative can be directly copolymerized with a suitable dihalogenated diaryl ether
 222 monomer unit to produce random (statistical) sulfonated poly(ether ether ketone) [36].
 223 Through careful control of the reaction stoichiometry, the sulfonate group can be
 224 introduced regiospecifically along the polymer backbone. This is achieved through the
 225 step-growth copolymerization reaction utilising sulfonated monomers [37].
 226 Electrophilic aromatic substitution reactions with various sulfonating agents can be
 227 used to produce sulfonated dihalogenated diaryl ketone or bisphenol monomer
 228 derivatives [38]. Nguyen et al. [39] synthesised a sulfonated di-halogenated diaryl
 229 ketone monomer by treating 4,4'-difluorobenzophenone with 25.3% fuming sulfuric
 230 acid, resulting in 100% yield and high purity disodium-3,3'-disulfate-4,4'-
 231 difluorobenzophenone (Figure 5).



232

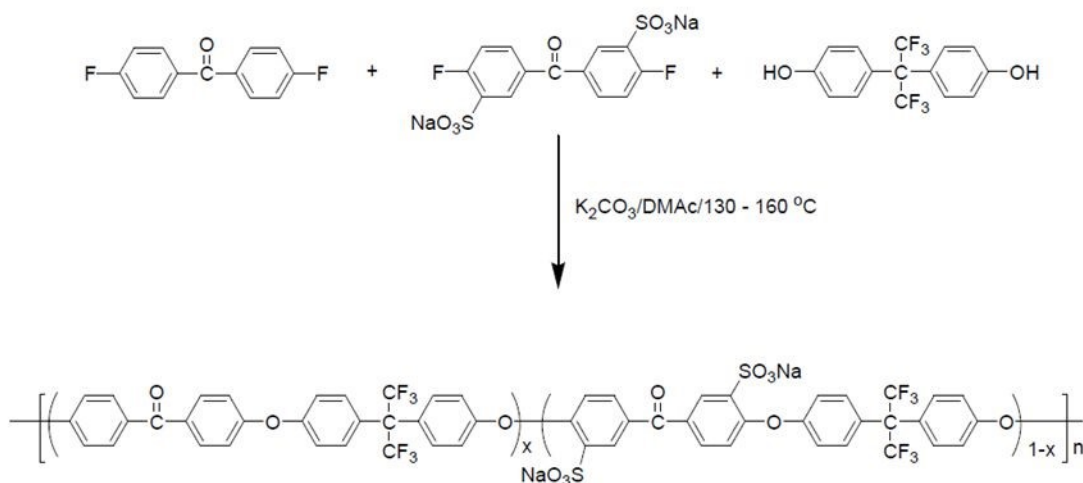
233 Figure 5. The reaction formula of a sulfonated di-halogenated diaryl ketone monomer [39].

234

235 A series of sulfonated poly(ether ether ketone) were produced by the base-catalysed
 236 nucleophilic aromatic polycondensation reaction of 4,4'-difluorobenzophenone and
 237 pure sulfonated monomer, disodium-3,3'-disulfate-4,4'-difluorobenzophenone with
 238 hexa-fluoro isopropylidene diphenol (Figure 6) [40]. High molecular weight polymers



239 that exhibit thermal stability up to 260 °C were produced. The resulting sulfonated
 240 poly(ether ether ketone)s were used as proton exchange membranes in fuel cells.



241

242 Figure 6. Reaction mechanism for preparation of Sulfonated poly (ether ether ketone) by the base
 243 catalyzed nucleophilic aromatic polycondensation [40].

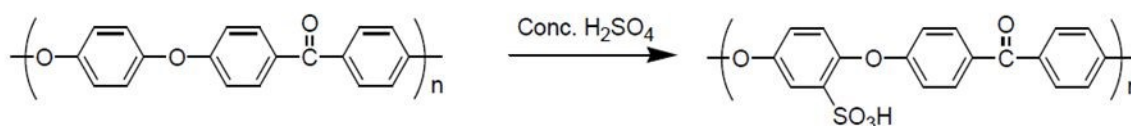
244

245 3.2 Direct post-polymerization sulfonation reactions with poly(ether ether 246 ketone)

247 Poly(ether ether ketone)s are highly effective polymers that are insoluble in the vast
 248 majority of organic solvents. Incorporating the sulfonic acid group along the polymer
 249 backbone of poly(ether ether ketone) reduces crystallinity and increases polymer
 250 solubility [41]. Direct sulfonation of poly(ether ether ketone)s using different sulfonating
 251 agents is not region-specific due to the lack of control over the degree and site of
 252 sulfonation during the sulfonation process [41]. Furthermore, polymer degradation and
 253 numerous side reactions have been observed. The electrophilic substitution reaction
 254 mechanism is used in the sulfonation of poly(ether ether ketone)s by sulfonating
 255 agents such as Sulfuric acid (H_2SO_4) as shown in figure 7. The ether linkage activates
 256 the polymer chain's phenyl rings for electrophilic substitution reactions, and the
 257 sulfonating group is introduced into the polymer chain's hydroquinone segment [42,
 258 43]. One sulfonic acid group is typically added per unit because the carbonyl group
 259 attracts electrons, which lowers the electron density of the other aromatic rings [41,
 260 44]. However, disulfonation reactions are possible at higher temperatures or for longer
 261 reaction time. Sulfonation reactions with poly(ether ether ketone)s are typically carried
 262 out in the presence of sulfonating agents like chlorosulfonic acid or sulfuric acid [45].



263 The reaction time, temperature, and acid concentration all influence sulfonation with
 264 sulfuric acid. In order to create polymers with different levels of sulfonation, Daud et al
 265 , [46] prepared sulfonated poly(ether ether ketone) from Victrex and 95-97%
 266 concentrated sulfuric acid and chlorosulfuric at room temperature acid to avoid PEEK
 267 polymer degradation and cross-linking reactions .The reaction was performed over a
 268 range of reaction times and degree of sulfonation of 80% was reported. In another
 269 study, Muthu Lakshmi et al., [47] investigated the effect of temperature and reaction
 270 duration on the degree of sulphonation of Gatone, as well as the characteristics of
 271 sulphonated polymers. Sulphonation was performed at 35-50 °C for 3-5 hours. The
 272 degree of sulphonation was between 50-80%. The sulfonated poly (ether ether ketone)
 273 derivatives were used in fuel cell and electrodialysis processes as electrochemical
 274 device.



275

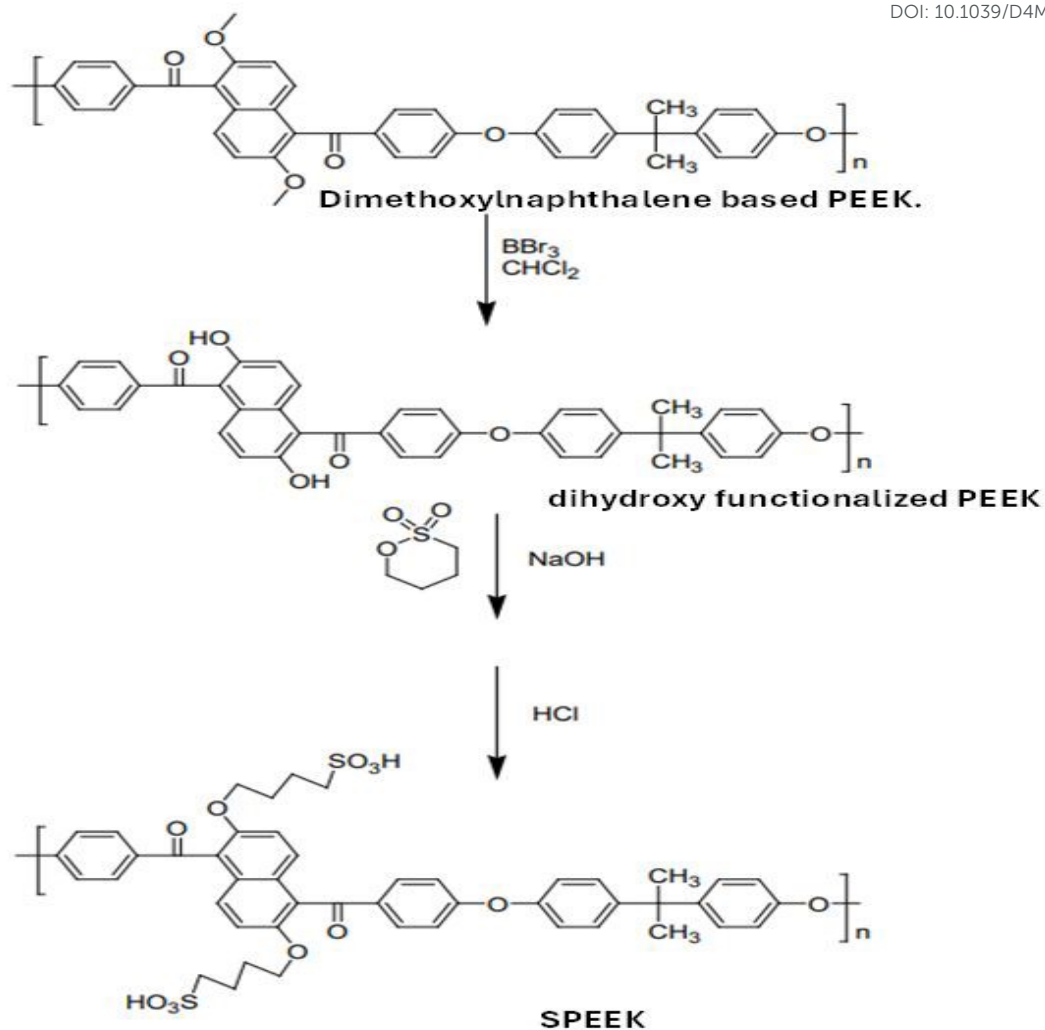
276 Figure 7. Sulfonation reactions of Gatone poly (ether ether ketone) [47]

277

278 To make it easier to incorporate the sulfonic acid group pendant into the polymer chain,
 279 standard organic reactions are commonly used to functionalize poly(ether ether
 280 ketone)s. Reactive sites in the polymer chain can be added either directly along the
 281 polymer backbone or by incorporating a suitable functional group pendant to the chain
 282 prior to the polymer precursor's sulfonation functionalization reaction.

283 Xu et al., [42] used dihydroxy functionalized poly(ether ether ketones) as substrates
 284 to synthesise a series of new sulfonated poly(ether ether ketones). The base catalyzed
 285 nucleophilic aromatic substitution polymerization method was used to create the
 286 corresponding dihydroxynaphthalene based poly (ether ether ketone) derivative.
 287 Sulfonated poly(ether ether ketone) was produced by the base-catalyzed nucleophilic
 288 reaction of dihydroxynaphthalene-based poly(ether ether ketone) with 1,4-butane
 289 sulfone (Figure 8). The resulting sulfonated poly (ether ether ketone) derivative
 290 exhibited high proton conductivity in DMFC applications.





291

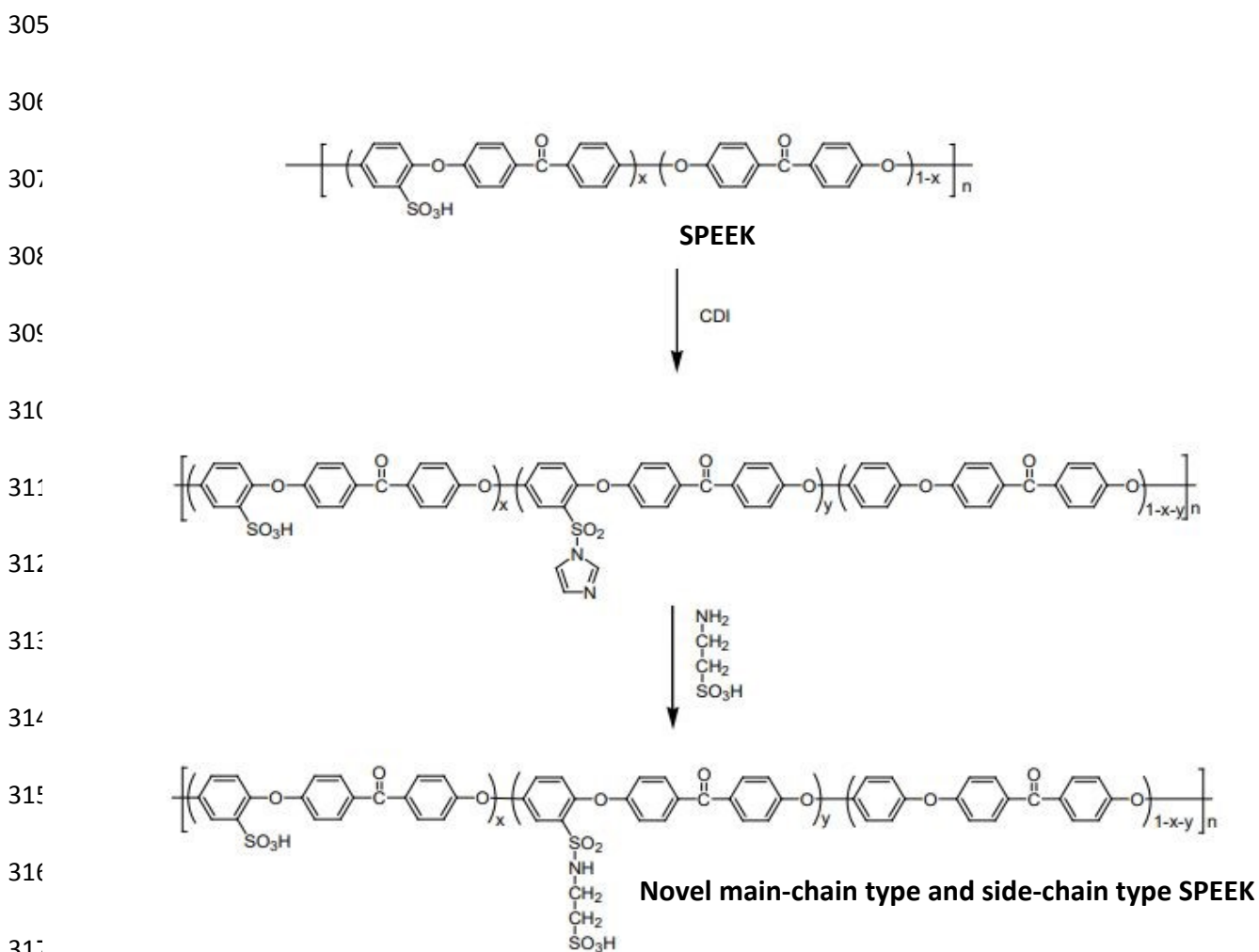
292 Figure 8. Nucleophilic reaction of dihydroxynaphthalene-based poly(ether ether ketone) with 1,4-butane
 293 sulfone [42]

294

295 Another synthetic method for creating sulfonated poly(ether ether ketone)s with the
 296 sulfonic acid group pendant to the polymer chain was created by Tsai et al., [48]. In
 297 order to produce pristine sulfonated poly(ether ether ketone), poly(ether ether ketone)
 298 was first treated with concentrated sulfuric acid. This was done by treating the resulting
 299 sulfonated poly (ether ether ketone) with 1,1'-carbonyl-diimidazole (CDI). Novel main-
 300 chain and side-chain sulfonated poly(ether ether ketone) with enhanced nano-phase
 301 separation morphology were formed after reaction with 2-aminoethanesulfonic acid
 302 (see figure 9). The addition of the new sulfonated group pendant to the polymer chain



303 resulted in well-defined nano-phase separation morphology and improved the properties of the proton exchange membrane in DMFC applications. View Article Online
DOI: 10.1039/D4MA00628C



319 Figure 9. Sulfonated poly(ether ether ketone) synthesis route using 1,1'-carbonyl-diimidazole (CDI) [48]

320

321 The sulfonic acid group can also be added to the poly(ether ether ketone) chain by the
322 thiol-ene reaction, which involves the following steps:

323 (i) The synthesis of a poly(ether ether ketone) precursor derivative with an
324 unsaturation site attached to the polymer chain.

325 (ii) The pendant site of unsaturation reacts with a mercapto compound containing a
326 sulfonate group using the classic thiol-ene reaction.



353 techniques, including blending and cross-linking, have been researched to create
354 effective SPEEK membranes [50].

355 **4.1 Membrane crosslinking**

356 **4.1.1 Electron beam (EB) radiation**

357 Radiation-induced crosslinking using electron beam (EB) is now extensively used for
358 processing polymer materials due to its inherent advantages over UV and thermal
359 curing methods. A radiation cross-linking strategy is a simple and efficient way to
360 reduce methanol permeability and improve membrane thermal and dimensional
361 stability, as well as mechanical properties, while maintaining proton conductivity [50].

362 Xiang et al [51] used a combination of cross-linking agents comprising
363 trimethylolpropane triacrylate (TMPTA), polyester acrylate, 2-(2-ethoxy-ethoxy)ethyl
364 acrylate (EOEOA), and 1,6-hexandiol diacrylate (HDDA) to introduce EB cross-linking
365 in the SPEEK structure. When different EB irradiation samples dosed at 6 kGy min⁻¹
366 were used, the degree of cross-linking and the density of the structure were directly
367 influenced by the exposure dose. Higher EB irradiation doses resulted in greater
368 thermomechanical and dimensional stability. They discovered that cross-linked
369 polymer membranes have greater cluster transition temperature than Nafion® 117
370 membrane, implying that cross-linked membranes may be more beneficial in high
371 temperature fuel cells than Nafion® 117 membrane. SAXS revealed ionic sites were
372 not deactivated by the cross-linking reaction, but rather increased proton conductivity,
373 especially at higher temperatures (90 °C). Moreover, greater proton conductivity and
374 dimensional stability at 80 °C and fully humidified conditions allowed for the
375 achievement of the maximum power density of 0.225 W.cm⁻² at a higher EB irradiation
376 dosage (200 kGy). Xiaomin et al [52] synthesised 1,6-bis (4-vinylphenyl) hexane
377 (BVPH), an unhydrolyzable cross-linker, to cross-link SPEEK membranes by EB
378 irradiation at room temperature in order to address challenges with dimensional
379 stability, mechanical strength, and methanol crossover. A higher degree of cross-
380 linking was achieved by adding the cross-linking agent (BVPH) at varying content
381 ranges of 5-15 wt% at a constant irradiation dose of 350 kGy and dose rate of 6 kGy
382 min⁻¹. Cross-linked membranes containing 15% BVPH outperformed pristine SPEEK
383 membranes in terms of dimensional and chemical stability, as well as mechanical
384 strength. Additionally, SPEEK containing 15% BVPH showed enhanced oxidative
385 resistance and tensile strength of 93 MPa (dry) and 38 h (3% H₂O₂, 2 ppm Fe²⁺, 80



386 °C). However, due to increased hydrophobicity and decreased water sorption and
387 active ionic sites, the proton conductivity of cross-linked SPEEK was slightly reduced.

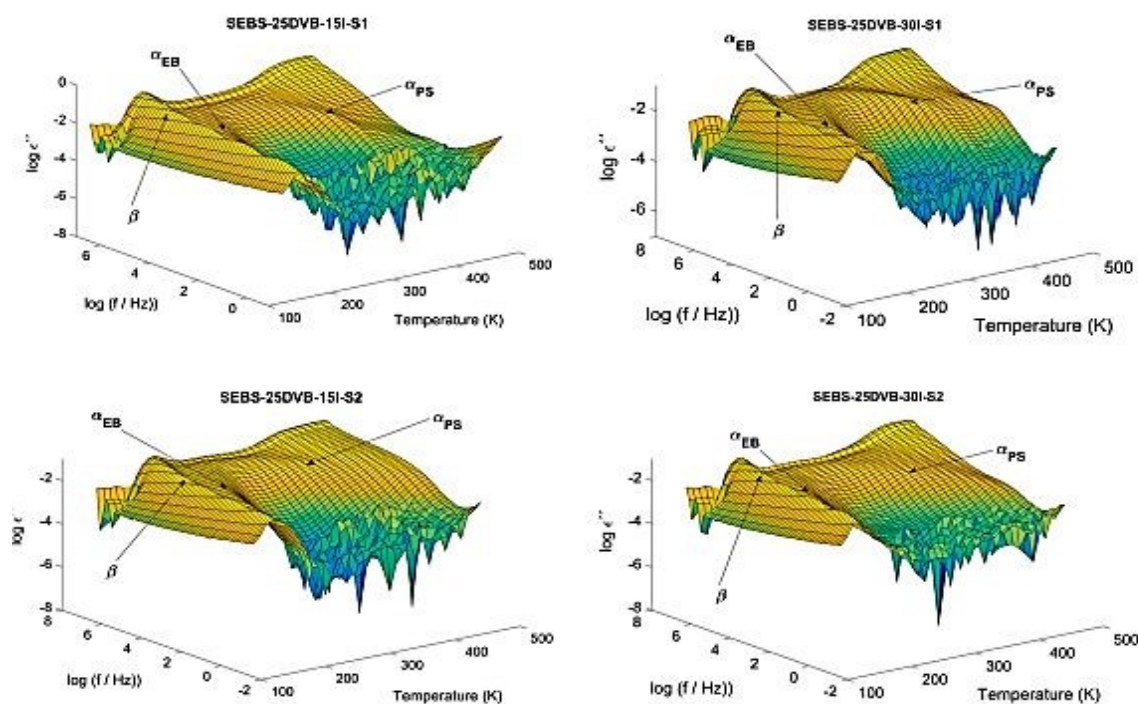
388 **4.1.2 UV radiation**

389 Prior to Hayes publishing a patent claiming that UV crosslinking increases the
390 environmental stability and lowers the gas permeability of polyimide materials, the
391 crosslinking of polymer materials by ultraviolet (UV) irradiation has been studied for a
392 long time but received little attention in the PEM research field [53]. Several polymer
393 membranes cross-linked by UV irradiation have since been studied in an effort to
394 improve the properties of the membrane.

395 Although there are many photo initiators and crosslinking agents on the market, they
396 can be highly unstable or very costly [54]. Chemical crosslinking can decrease the
397 efficiency of polymer chain packing, leading to an increase in gas permeability and
398 potential modifications in the properties of membranes [55]. Consequently, most
399 researchers have focused their attention on adding the photo initiator and/or suitable
400 crosslinking sites to the polymer backbone. The UV-crosslinked hybrid SPEEK
401 membrane, which is combined with biodegradable polymer, reduces the polymer
402 chains' elasticity by forming a denser network. Ramly et al., [56] studied SPEEK with
403 methylcellulose (MC) and UV radiation, using benzoin ethyl ether (BEE) as a photo
404 initiator. Increased hydrophilicity was achieved through radiation-induced
405 demethylation, chain cleavage, acid group formation, and carbonyl in MC. After the
406 non-crosslinked membrane was crosslinked with BEE under UV light for 30 minutes,
407 the proton conductivity at 30 °C increased from 0.004 S cm⁻¹ to 0.008 S cm⁻¹. The UV
408 membrane improved dimensional stability after crosslinking because of its denser
409 structure. Teruel-Juanes et al., [57] carried out the crosslinking reaction first by UV
410 irradiating polystyrene-ethylene-butylene block copolymers (SEBS) with DVB, as
411 opposed to first performing the sulfonation and then the crosslinking. This was
412 followed by a post-sulfonation of the hardened membranes in trimethylsilyl
413 chlorosulfonate solutions in 1,2-dichloroethane (DCE). The dielectric relaxation
414 spectrum (Figure 11) revealed two main relaxations that corresponded to the glass
415 transitions of the ethylene-butylene (EB) and styrene (S) blocks, as well as sub-T_g
416 intramolecular non-cooperative dielectric relaxation. In addition to having an impact on
417 the fragilities of both styrene (S) and ethylene-butylene (EB) blocks, the photo-
418 crosslinking and post-sulfonation processes also have an effect on the entire dielectric



419 relaxation spectrum. They concluded that the behaviour of the membranes can be
 420 estimated and reengineered based on modifications to the desired cell performance
 421 thanks to a correlation found between relaxation processes and membrane
 422 performance in H₂/O₂-PEM single cells.



423
 424 Figure 11: Dielectric relaxation spectrum [57].

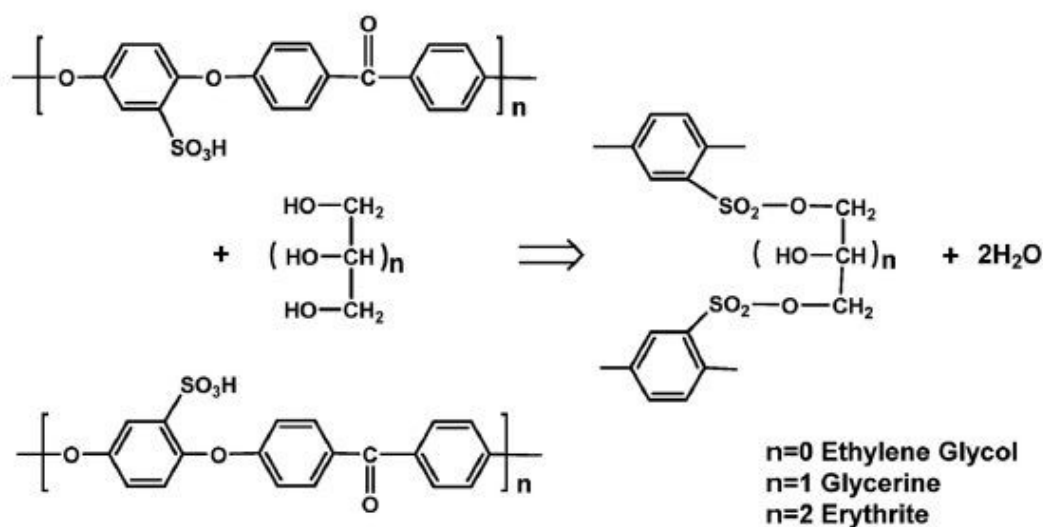
425 4.1.3 Chemical cross-linking

426 Crosslinking of polymers can also be initiated by adding chemical additives during the
 427 membrane casting process. A wide range of unique additives, such as sulfonic acid
 428 groups and "free" hydrocarbon locations on the polymer chain, are identified in the
 429 literature, each with a unique crosslinking mechanism.

430 Polyatomic alcohols such as glycerol, ethylene glycol, and meso-erythrite can be used
 431 as crosslinking agents to increase or maintain the SPEEK membrane's flexibility
 432 (Figure 12). This is due to the fact that sulfone bond created by thermal crosslinking
 433 between two sulfonic acid groups are less flexible than the sulfonic ester bond created
 434 by condensation with polyatomic alcohol. Conductivity is enhanced by the flexibility of
 435 the macromolecular chains, which enable them to align into hydrophilic and
 436 hydrophobic domains [58]. Kumari et al., [59] reported on the effect of polyatomic
 437 alcohol linker length. They used ethylene glycol (PEG) with different molecular weights



438 (MW/Da: 200 to 10000) and measured the effect of the molecular weight on the
 439 membrane's final properties. The authors reported that PEG 400 could form many
 440 small hydrophilic and hydrophobic clusters, which were more feasible than larger
 441 clusters formed by PEG with a MW less than 600. They made this discovery using
 442 atomic force microscopy (AFM) and small-angle X-ray scattering (SAXS). The results
 443 also demonstrated that there was an optimal linker length for stacking macromolecular
 444 chains into hydrophobic and hydrophilic domains.



445

446 Figure 12: Reaction scheme of SPEEK cross-linked with polyatomic alcohol [42]

447 The diol crosslinking agents' flexibility was also examined by Gupta et al in a different
 448 study [60]. To crosslink the SPEEK membrane, cyclohexane di-methanol (CDM) was
 449 utilised as the stiff crosslinking reagent and PEG (MW 200) as the flexible crosslinking
 450 reagent. According to their report, the ideal ratio of polymer to crosslinker was
 451 determined to be 3:1 after conducting conductivity and water uptake experiments with
 452 various crosslinking agent ratios. Moreover, membranes crosslinked with the stiff CDM
 453 exhibited inferior properties in comparison to those crosslinked with the flexible
 454 crosslinker PEG. Therefore, the crosslinkers' flexibility is another factor to consider
 455 when crosslinking SAP.

456

457



458 **4.2 SPEEK blend polymer membrane**

459 Blending is a simple method for defining and adjusting phase separation in the
460 microstructure of homopolymers, provided the second polymer is completely
461 compatible with the primary polymer [61]. Hydrogen bonds and ionic interactions, which
462 are the most common physical interactions between polymers, can be used to reinforce
463 blend membranes.

464 **4.2.1 Acid-base polymer blend**

465 An acid-base blend membrane is formed when benzimidazole side groups are
466 introduced to the polysulfone backbone and blended with SPEEK [62]. The
467 benzimidazole group uses basic nitrogen as a medium to transfer protons between the
468 sulfonic acid groups of SPEEK, supporting both the hopping-type and vehicle-type
469 mechanisms. The blend membrane outperforms the Nafion[®] and pristine SPEEK
470 membranes in PEMFC between 60 and 100 °C [63]. Numerous researchers selected
471 Poly(amide imide) (PAI) to blend with SPEEK due to the effectiveness of sulfonated
472 polyimides in preventing methanol diffusion. The addition of PAI to the membrane
473 structure reduces the swelling ratio and methanol permeability while increasing
474 mechanical, thermal, and oxidative properties. As expected, as the PAI content was
475 increased, a decrease in proton conductivity was observed. To improve mechanical
476 properties, Raja et al., [64] loaded BaCeO₃ nanoparticles in the SPEEK/poly (amide-
477 imide) (PAI) matrices. The addition of BaCeO₃ nanoparticles improved conductivity, ion
478 exchange, and water uptake (WU) properties while maintaining controlled stability due
479 to the good interfacial interaction between nanoparticles and polymer. The polymer was
480 reported to have stronger methanol barrier properties, making them suitable for DMFC.

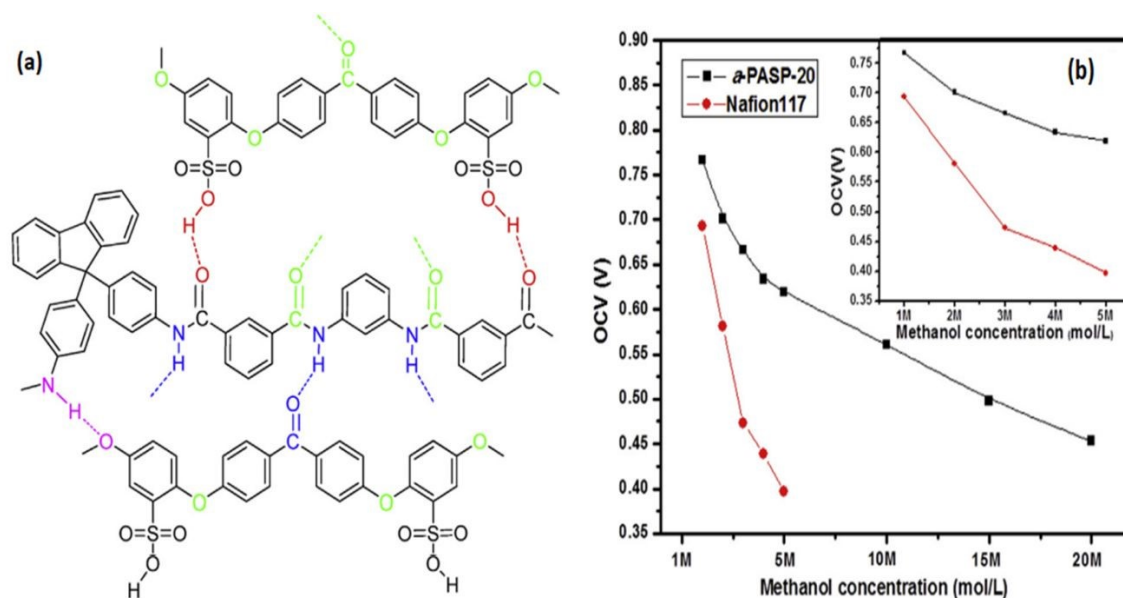
481 **4.2.2 Acid-acid polymer blend**

482 Introducing hydrogen bonds between polymer chains in a blend PEM is an appealing
483 approach to reduce methanol permeability and improve the durability of DMFC. Fully
484 aromatic polyamide (fa-PA) was blended with 76% sulfonation degree into SPEEK by
485 Li et al [65]. There are plenty of electronegative sites, such as carbonyl, amine, and
486 sulfonate groups, which can form dense morphology, to establish H-bonds between
487 polymer chains, as shown in Figure 13a. In comparison to pristine SPEEK, the fa-PASP-
488 20 (20 weight percent fully aromatic polyamide) showed improved mechanical strength
489 and swelling behaviour at 25 °C. Furthermore, in an aqueous methanol solution (2 M)
490 at room temperature, faPASP-20 demonstrated relatively low methanol permeability of



491 $1.29 \times 10^{-7} \text{ cm}^2 / \text{s}$, while SPEEK's values were $3.06 \times 10^{-7} \text{ cm}^2 / \text{s}$. The open circuit voltage
 492 (OCV) values for fa-PASP-20 and Nafion® 117 as a function of methanol concentration
 493 are shown in Figure 13b, indicating that the blend PEM has good methanol resistance
 494 even at high concentrations.

495



496

497 Figure 13: Expected hydrogen bonding between the blend of sulfonated poly (ether ether ketone) with
 498 fully aromatic polyamide (fa-PA), and (b) OCV of fa-PASP-20 blend and Nafion® 117 membranes at
 499 different methanol concentrations [65].

500

501 Haragirimana et al., [66] created a synergistic effect in SPEEK and SPAES by using
 502 acid-acid blending and sulfone bridges between sulfonic acid groups and electron-rich
 503 phenyl units. In their study, they fabricated a series of PEEK/SPAES polymer blends
 504 through a three-component system. Ductile and dense membranes were successfully
 505 fabricated through simple solution mixing and casting due to the excellent compatibility
 506 and fine dispersion of both copolymers inside the membrane. The incorporation of
 507 SPAES into SPEEK had a significant positive effect on the control of membrane water-
 508 swelling behaviour and oxidative stability, particularly at high temperatures. This
 509 resulted from the interfacial interactions (π - π interactions) and strong hydrogen bond
 510 formation between the SPAES and SPEEK chains.



511 **4.2.3 Blending with Perfluorosulfonic acid (PFSA) membrane.**

512 PEMs can be made from PFSA polymers blended with SPEEK. The SPEEK nanofiber
513 mat was first electrospun, followed by impregnation with PFSA polymers [67].
514 Dimensional stability and mechanical properties improved, but proton conductivity
515 decreased when compared to the pristine membrane. Fluoropolymers, such as poly(-
516 vinylidene fluoride) (PVDF) or poly(vinylidene fluoride-cohexafluoropropylene) (PVDF-
517 HFP), can simply be blended with SPAEKs or SPAESs to create composite
518 membranes [68]. The addition of PVDF or PVDFHFP decreased proton conductivity
519 while improving water uptake, swelling ratio, and methanol barrier properties.

520 In another fascinating study, Nayak et al.,[69] combined non-fluorinated blend
521 membranes and SPEEK with fluorinated blend membranes. Sulfonated poly (ether-
522 ether-ketone)/poly (vinylidene fluoride-co-hexafluoro propylene)/Silica (SPEEK/PVdF-
523 HFP/SiO₂) composite proton exchange membranes were developed for fuel cell
524 applications. The SiO₂ (7.5 wt.%) polymer membrane of SPEEK (80 wt.%) / PVdF-
525 HFP (20 wt.%) demonstrated the highest proton conductivity value of 8×10^{-2} S.cm⁻¹.
526 Additionally, a maximum power density of 1.5 mW.m⁻² was reported. According to this
527 study, a different PEM may be possible if SiO₂ is added to polymer composite
528 membranes.

529 A high ionic conduction sulfonated poly(ether ether ketone)/poly(vinylidene fluoride)
530 (SPEEK/PVDF) blend membrane doped with boron phosphate (BP) was developed
531 by Cali et al. [70]. SPEEK/ PVDF/10BP had the highest current density (0.4 A.cm⁻²)
532 and power density (0.242 W.cm⁻²) at 0.6 V. The proton conductivity of the
533 SPEEK/PVDF/10BP sample was measured at 80 °C to be 39 mS.cm⁻¹. The addition
534 of both the boron phosphate and the SPEEK/PVDF mix membrane resulted in
535 promising results for future fuel cell operations.

536 **4.2.4 Blending with non-fluorinated membrane**

537 Wang et al. reported the preparation of PVA-SSA/SPEEK composite membranes from
538 sulfosuccinic acid crosslinked with polyvinyl alcohol (PVA-SSA) [71]. In comparison
539 to the pristine membrane, the blended polymers ion exchange capacity (IEC) and
540 water uptake (WU) were found to be lower, despite their high tensile strength PVA-
541 SSA reaction may be hindered by low DS and PVA crosslinking when SPEEK is
542 present. The presence of SPEEK in the blend, as well as the crosslinking of PVA with
543 SSA, appear to result in greater thermal stability. When hydrated, PVA-SSA/SPEEK



544 (70:30) was found to have a proton conductivity of 0.070 S.cm^{-1} . A blend of SPEEK
545 and sulfonated poly (phthalazinone ether sulfone ketone) (SPPEsk) was developed
546 by Liu et al., [72]. Excellent water absorption and a low swelling ratio are features of
547 the reported SPPEsk/SPEEK membrane. At $80 \text{ }^\circ\text{C}$, the blend membrane's proton
548 conductivity was reported to be 0.212 S.cm^{-1} .

549 **4.3 The modification of SPEEK membranes with other polymers**

550 In most polymers, carbon atoms are covalently bound to other elements like hydrogen,
551 oxygen, or nitrogen. These organic molecules can be thought of as polymers. Hence,
552 combining a polymer with SPEEK can result in the formation of acid-base interactions
553 or hydrogen bonds between polymer chains, which can drastically alter the mixture's
554 characteristics. SPEEK combined with other polymers is a technique commonly
555 utilized in composite membranes manufacture, offering excellent proton conductivity
556 and acceptable mechanical qualities. Blends of SPEEK with various polymers,
557 including polyacrylonitrile (PAN) [73], polybenzimidazole (PBI) [74], poly(ether
558 sulfone) (PES) [75], polyimide (PI) [76], polyphenylene oxide (PPO) [77],
559 polytetrafluorethylene (PTFE) [78], vinylidene fluoride [79], polyvinylpyrrolidone (PVP)
560 [80] and poly(tungstophosphoric acid (TPA) [81]. According to Peng et al., the
561 performance of SPEEK membrane can be enhanced by altering its microstructure
562 using either dibutyl phthalate (DBP) porogen or Nafion resin, which is applied as a
563 layer over polypropylene (PP). It has been reported that a modified membrane
564 structure consisting of the SPEEK membrane coated with polydopamine (PDA) layers
565 improves mechanical strength and selectivity. All of these methods improve
566 performance and point to the use of composite SPEEK membranes in PEMFC
567 applications.

568 Recently, phosphonate membranes have received increased attention as potential
569 replacement for PEMFC applications. Phosphorylated polysulfone (PPSU-As) in the
570 acid form with degrees of phosphonation (DP) of 0.4, 0.75, and 0.96 was successfully
571 prepared and blended by Abu-Thabit et al., [82] using SPEEK with a DS of 0.75 . The
572 phosphoryl group ($-\text{PO}_3\text{H}_2$) could form strong hydrogen bonds with acidic SPEEK
573 polymers, reducing swelling while sacrificing minimal proton conductivity. When
574 compared to pure SPEEK, the blend SPEEK/PPSU membrane demonstrated lower
575 methanol permeability, increased mechanical strength, and water uptake without
576 sacrificing proton conductivity. The blend membrane (30PPSU-A-0.96) performed



577 better in terms of proton conductivity than the pristine SPEEK membrane. The
578 maximum proton conductivity of 0.124 S.cm^{-1} was reached at $120 \text{ }^\circ\text{C}$, where this
579 performance was sustained. Sultan et al., [83] created a novel hybrid membrane poly
580 (trimellitic anhydride chloride-co-4,4'-methylenedianiline) (SPEEK/PTCMA) with
581 PTCMA loadings ranging from 10% to 50% with a DS of 53%. SPEEK/PTCMA (50
582 wt.%) exhibited lower water uptake of 11% at room temperature, because of the acid-
583 base interaction of amine and sulfonated groups. At $90 \text{ }^\circ\text{C}$, the composite membrane
584 SPEEK/PTCMA (20 wt.%) demonstrated higher proton conductivity of 0.004 S.cm^{-1} .
585 The addition of PTCMA improved proton conductivity because the nitrogen atom of
586 PTCMA can be protonated and contribute to proton transfer. Overall, the findings
587 demonstrated that the proton conductivity value decreased as the PTCMA content
588 increased. In turn, this lowers the amount of sulfonic acid groups in the composites,
589 increasing their crystallinity and thereby decreasing water uptake a crucial stage in
590 proton transfer.

591 Han et al., [84] ., created SPEEK/PBI composite membranes by dissolving the two
592 polymers in DMAc before casting the membrane . The interaction of the -NH groups
593 in PBI and the -SO₃ groups in SPEEK results in the formation of a three-dimensional
594 network polymer structure that is advantageous for proton transport. The PEM
595 demonstrated excellent proton conductivity performance, with a value of 0.14 S cm^{-1}
596 at $80 \text{ }^\circ\text{C}$, comparable to Nafion 117 (0.142 S cm^{-1}). The permeability of methanol is
597 also as low as $2.38 \times 10^{-8} \text{ cm}^2 \cdot \text{s}^{-1}$, which is much lower than that of Nafion. Aside from
598 mechanical properties, thermal stability is also important. Such a polymer membrane
599 design is successful and close to being used in DMFCs. Wei et al., [76] proposed a
600 PI/SPEEK/PI nanofiber composite membrane with a sandwich structure and simple
601 fabrication processes. The formation of an acid-rich layer and the solid support of PI
602 nanofibers on the SPEEK matrix resulted in significantly improved proton
603 performance. Due to the acid-base interaction between tertiary amide groups and
604 sulfonated groups, the novel hybrid membranes PI/SPEEK with PI loadings of 3% and
605 PI/SPEEK/PI with PI loadings of 1.5% had lower methanol permeability than SPEEK
606 membranes. The sandwiched membranes demonstrated excellent conductivity of
607 0.178 S.cm^{-1} at $60 \text{ }^\circ\text{C}$, which is noticeably higher than that of neat SPEEK membrane.
608 The fuel cell's performance can reach 0.152 W.cm^{-2} . The swelling ratio and water
609 uptake of the PI/SPEEK nanofiber composite membrane are 24.3% and 50.8%,



610 respectively, at 60 °C and 100% RH, demonstrating the sandwiched PEM's excellent
611 dimensional stability. The excellent results of the polymers indicate that the PI/SPEEK
612 membrane is a promising candidate for commercial PEM with balanced proton
613 conductivity, stability, and durability. The sandwich-structure membrane concept can
614 also be applied in other areas such as vanadium redox flow battery, gas separation
615 membrane, and so on.

616 Another promising membrane with strong chemical resistance and high hydrophilicity
617 is chitosan. The combination of SPEEK and the natural polymer chitosan was
618 suggested by Hidayati et al. [85]. Chitosan with low methanol permeability and good
619 conductivity has been treated with SPEEK to eliminate hydroxyl and amine groups.
620 The SPEEK/Chitosan composite membrane showed enhanced methanol permeability
621 of $2.46 \times 10^{-6} \text{ cm}^2 \cdot \text{s}^{-1}$ at room temperature when compared to pristine chitosan.
622 SPEEK/Chitosan IEC values are higher, resulting in high proton conductivity. It was
623 reported that SPEEK/Chitosan produced contrasting results for DMFC, implying that
624 more research is needed.

625 **5. Modification of SPEEK membranes with inorganic materials**

626 SPEEK polymer modification with inorganic materials such as silica, clays, metal
627 oxides, HPA, carbon nanotubes, and others has recently been investigated in fuel cell
628 applications. The incorporation of inorganic substances into PEMs is known to improve
629 proton conductivity, mechanical strength, and composite membrane durability [86].
630 While simultaneously enhancing the mechanical and thermal stabilities of the
631 composites, Inorganic elements can reduce methanol crossover and excessive water
632 swelling [87]. The various types of additives in SPEEK, such as graphene, silica, metal
633 oxides, Heteropolyacids (HPAs), carbon nanotubes, Metal organic framework (MOFs)
634 and clay will be thoroughly discussed in these subtopics. The influence of different
635 additives on the SPEEK matrix; and its impact on the SPEEK performance with focus
636 on fuel cells are shown in Table 1.



TABLE 1: THE INFLUENCE OF DIFFERENT ADDITIVES ON THE SPEEK POLYMER MATRIX

Additive Type	Temperature (°C)	IEC (meq g ⁻¹)	Water Uptake (%)	Proton conductivity (S cm ⁻¹)	Power density (mW cm ⁻²)	Ref
SiO ₂ @CNT	25	-	43	4.1x10 ⁻²	-	[88]
SWCNT-fly ash	90	1.59	27.3	3.4x10 ⁻²	672	[89]
SsCNT-5	90	2.19	43.85	4.31x10 ⁻²	-	[90]
CCNF	80	-	32.3	5.6x10 ⁻²	-	[91]
β-CD-DHNTS/HPW	-	1.04	30	9.0x10 ⁻²	-	[92]
Cs-HPAs	80	-	40	2.25x10 ⁻³	247	[93]
Pt-Cs _{2.5} H _{0.5} PW ₁₂ O ₄₀	60	1.96	46	6.82x10 ⁻²	-	[94]
PEOS/PWA/SiO ₂	100	-	-	6.25x10 ⁻³	25	[95]
Cs-TPA	80	1.5	37	1.3x10 ⁻¹	-	[96]
Pd-GO-L-Tyr	-	2.05	50.6	2.56x10 ⁻³	-	[109]
PANI-GO	-	1.83	40	8.4x10 ⁻³	13.51	[97]
SPBI/PrSGO	90	2.02	-	1.7x10 ⁻¹	820	[98]
SPVdF-HFP-SiO ₂	90	1.83	36.5	7.9x10 ⁻²	110	[99]
HPW@KMSNs	60	-	31.5	2.43x10 ⁻¹	-	[100]
PVA/TEOS	80	2.02	76	8.1x10 ⁻²	336	[101]
IL/SHMO	200	-	-	4.6x10 ⁻³	-	[88]
Bentonite/clesite30	80	-	18.4	1.24x10 ⁻⁵	-	[102]
fGO/halloysite	-	0.35	-	4.7x10 ⁻⁴	72.2	[103]
SiO ₂ -montmorillonite	100	-	25	1.58x10 ⁻¹	-	[104]
BaZro ₃	90	1.96	41.5	3.12x10 ⁻¹	183	[105]
Al-CeZrO ₄ /HPW	80	1.65	8.1	1.3x10 ⁻³	1001	[106]
NBO	90	1.80	38.4	2.9x10 ⁻²	601	[107]
ZCO	90	1.46	20.3	2.0x10 ⁻²	-	[108]
HPW@ML	60	1.54	50	1.36x10 ⁻¹	-	[109]
MOF-C-SO ₃ H	80	1.63	28.7	1.1x10 ⁻¹	82	[110]
Co-MOF-74/[IM ₂][H ₂ PO ₄]	120	6.5	90	2.6x10 ⁻²	-	[111]
Cu-MOF	80	2.46	36.7	7.1x10 ⁻²	-	[112]
ZIF-8/CNT	120	1.48	40.2	5.0x10 ⁻²	-	[113]
ZIF-67	120	0.3	40	1.4x10 ⁻²	28	[114]

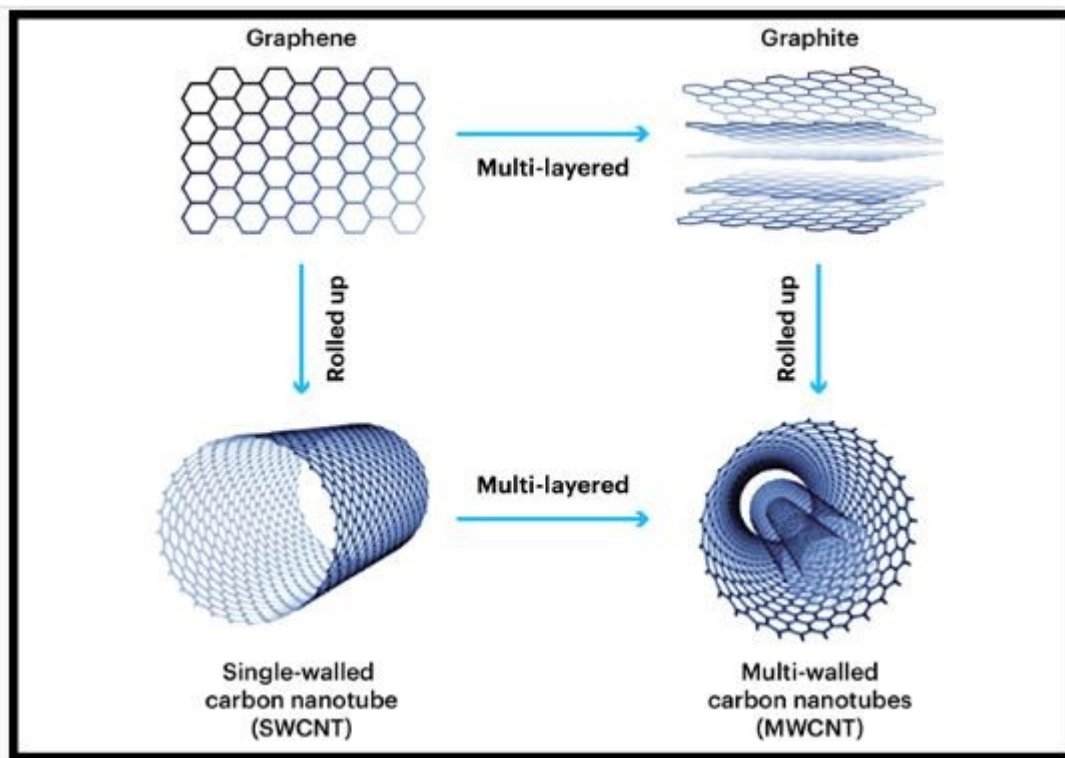
637

638 5.1 Carbon nanotubes as fillers for SPEEK membrane

639 CNTs are one-dimensional tubular-like hexagonal graphene sheets formed by sp²
640 bonds between carbon atoms. CNTs have extremely high mechanical properties due
641 to this bonding structure, which is stronger than the sp³ bonds found in diamond.
642 CNTs can be single-walled (SWCNT) or multiwalled (MWCNT), with diameters ranging
643 from 1 nm to more than 100 nm, as shown in Figure 14. The rolling-up direction of the
644 graphene sheet has a significant impact on the CNT's electrical conductivity. This is
645 due to the fact that the chirality vector describes the hexagonal carbon atom lattice.
646 However, due to their higher surface defects and lower electrical conductivity,



647 MWCNTs are preferred over SWCNTs for use in PEMs [115]. Due to their stiffness,
 648 low density, high aspect ratio, and optical qualities, as well as their exceptional tensile
 649 strength of roughly 63 GPa, which is 50 times stronger than steel, carbon nanotubes
 650 (CNTs) have received a lot of attention as a reinforcing material for polymers [116].



651

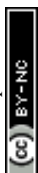
652 Figure 14: Single walled and multiwalled carbon nanotubes [116].

653 Carbon nanotubes (CNTs) are a cutting-edge nanomaterial for the production of
 654 exceptional polymer composites. Recently, SPEEK has employed CNTs as fillers to
 655 address DS-dependent issues. Nonetheless, CNTs have a negative impact on proton
 656 conductivity because they are an electron conductor rather than a proton conductor,
 657 which may pose a significant risk of short-circuiting on PEMs in fuel cells. Cui et al.,
 658 [88] successfully prepared silica-coated CNTs (SiO_2 @CNTs) by a simple sol-gel
 659 method, and subsequently applied as a novel additive to SPEEK-based composite
 660 membranes, which are enhanced by silica's exceptional water retention and electronic
 661 shield properties. Not only did the hydrophilic and insulated silica coating on the CNTs'
 662 surface prevent short circuiting, but it also enhanced the CNTs' interfacial contact with
 663 the SPEEK matrix, promoting the CNTs' uniform dispersion. Moreover, the methanol
 664 permeability of the SPEEK/ SiO_2 @CNT composite membrane with a SiO_2 @CNT
 665 loading of 5% was nearly one order of magnitude lower at $4.22 \times 10^{-8} \text{ cm}^2 \cdot \text{s}^{-1}$ as

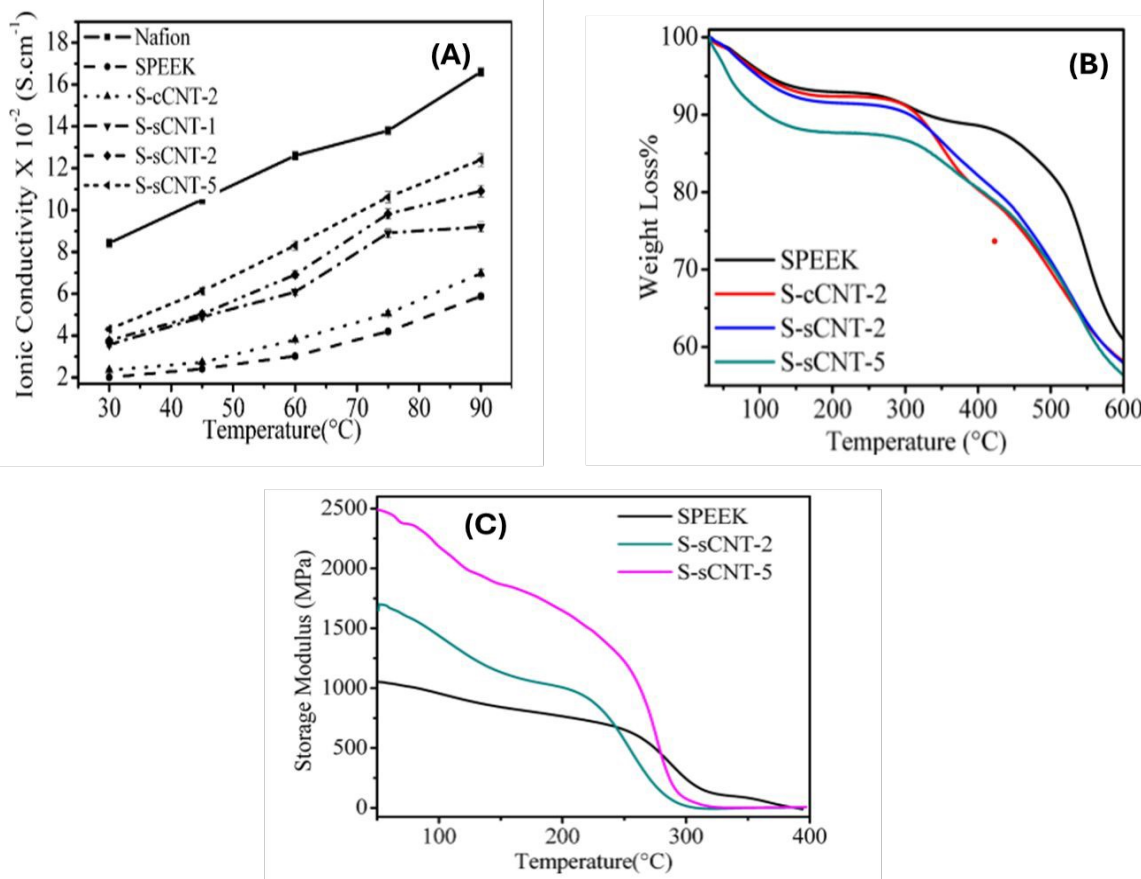


666 compared to the pure SPEEK membrane ($3.42 \times 10^{-7} \text{cm}^2 \cdot \text{s}^{-1}$). At room temperature,
667 the proton conductivity remained greater than $10^{-2} \text{S} \cdot \text{cm}^{-1}$. The obtained results
668 demonstrate that SPEEK/SiO₂@CNT membranes can be used as high-performance
669 PEMs in direct methanol fuel cells. Sivasubramanian et al., [89] successfully
670 synthesised Sulfonated poly (ether ether ketone) (SPEEK)-based polymer
671 nanocomposite membranes comprising single-walled carbon nanotubes (SWCNTs)
672 and fly ash as inorganic fillers using the solution casting method. The degree of
673 sulfonation in poly (ether ether ketone) was evaluated using proton nuclear magnetic
674 resonance spectroscopy and found to be 64%. They investigated and analyzed the
675 produced membranes' physicochemical characteristics and potential for fuel cell
676 applications. At 90°C, the SP-CNT-FA-8 membrane had the maximum proton
677 conductivity ($3.4 \times 10^{-2} \text{S cm}^{-1}$), whereas the pristine membrane had a conductivity of
678 $3.1 \times 10^{-2} \text{S cm}^{-1}$. Apart from their favourable proton conductivity, it was also reported
679 that the electrolyte membranes demonstrated remarkable thermal and mechanical
680 stability. These findings suggest that the composite membranes utilizing SPEEK,
681 SWCNT, and fly ash could be promising electrolyte membrane options for fuel cell
682 applications.

683
684 Gahlot et al., [90] used solution casting to create functionalized carbon nanotubes (f-
685 CNT) that are aligned electrically with SPEEK. The CNTs were functionalized via
686 carboxylation and sulfonation. During the membrane's drying process, the CNTs were
687 aligned using a constant electric field of $500 \text{V} \cdot \text{cm}^{-1}$. To determine whether they have
688 the potential for direct methanol fuel cell application, the proton conductivity and
689 methanol crossover resistance were assessed at temperatures ranging from 30 °C
690 to 90 °C. According to the findings, addition of aligned carbon nanotubes (CNTs)
691 reduces the permeability of methanol while increasing the ion-exchange capacity,
692 water retention, and proton conductivity. The highest proton conductivity (4.31×10^{-2}
693 $\text{S} \cdot \text{cm}^{-1}$) was observed in the SsCNT-5 nanohybrid PEM, which exhibited a higher
694 resistance to methanol crossover. As the concentration of s-CNTs in the SPEEK
695 matrix increased, so did the storage modulus (Figure 15). The S-sCNT-5 membrane
696 had the highest modulus value of 2503 MPa, which is nearly 2.4 times higher than the
697 SPEEK membrane. The increase in storage modulus of S-sCNT membranes indicates
698 strong bonding due to the presence of a common sulfonic acid group in CNT and



699 PEEK, as well as the effect of electric field on CNT alignment in the SPEEK matrix.
 700 The electrically aligned functionalized CNT/SPEEK membranes outperformed the
 701 randomly aligned composite membranes.



702

703 Figure 15: (a) Proton conductivity vs temperature (b) TGA thermographs and (c) DMA of SPEEK, S-
 704 sCNT-2, and S-sCNT-5 membranes[90].

705

706 Zhao Guodong et al., [91] prepared a composite membrane for use in PEMs by
 707 incorporating continuous carbon nanofibers (CCNFs) into SPEEK. The (CCNFs) were
 708 evenly distributed in an electrolyte polymer membrane after being easily blended into
 709 SPEEK matrix. The characterization of the composite membranes shows that all
 710 dense composite membranes have low methanol permeability, good proton
 711 conductivity, high mechanical performance, and excellent water swelling. The
 712 composite membrane containing 0.51 weight percent (wt%) CCNFs was fully hydrated
 713 and had a proton conductivity of 0.056 S.cm⁻¹ at room temperature. Moreover, 1.5
 714 times the relative selectivity of a pure SPEEK membrane was observed in the hybrid
 715 membrane containing 2.52 weight percent CCNFs. These results showed that

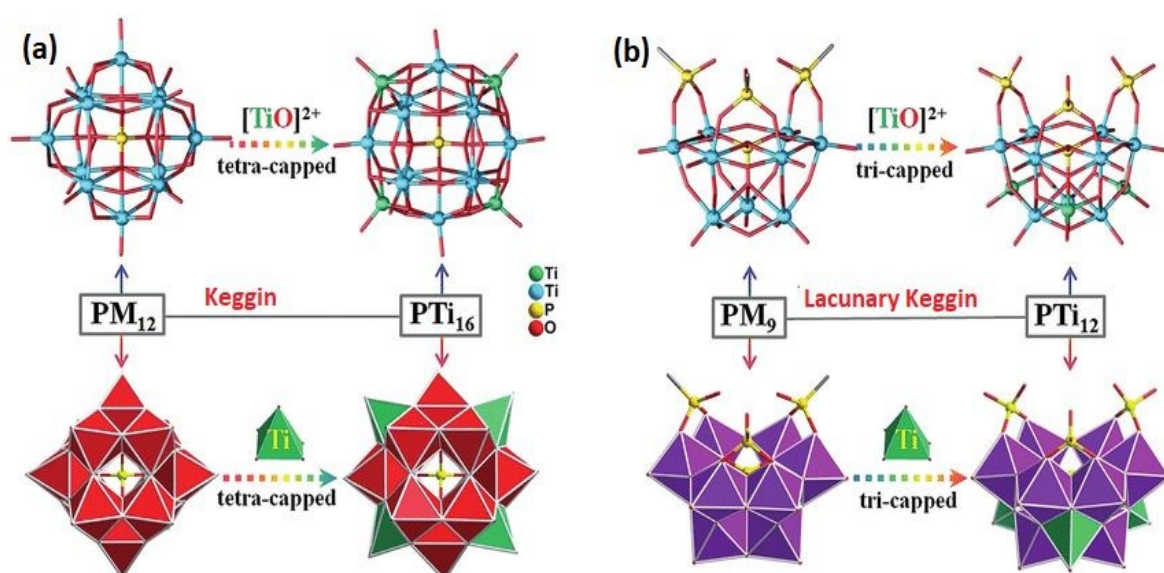


716 polyelectrolyte membranes for fuel cells with CCNF support (SPEEK) are a promising
 717 option.

718 5.2 Heteropolyacids (HPAs) as fillers for SPEEK membrane

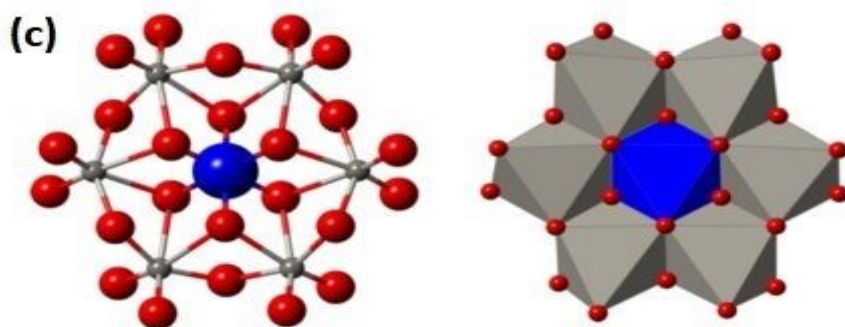
719 The HPAs are highly conductive and thermally stable crystalline inorganic materials.
 720 HPAs salts are composed of MO_x polyhedral, where M represents polyatoms such as
 721 Tungsten (W), Molybdenum (Mo), Niobium (Nb), Tantalum (Ta), and Vanadium (V),
 722 and x represents heteroatoms such as Silicon (Si), Phosphorus (P), Iron (Fe), and
 723 Cobalt (Co) through an oxygen atom coordination bridge [117]. They are typically
 724 distinguished by Wells-Dawson, Keggin, or lacunar structural configurations (Figure
 725 16). Different salts with different structures and properties can be formed by changing
 726 the central metal ion and addenda atoms. HPAs are soluble in polar solvents, where
 727 they form the Keggin structure ($XM_{12}O_{40}$), which is a heteropolyacid anion structure
 728 with a condensation ratio of 1:12. The high acidity of HPAs is attributed to the
 729 polyanion's large size, which results in a low delocalized charge density. Chemical
 730 analysis, ion selective membranes, sensors, chemical cleaners, catalysts, and
 731 additives in fuel cell component materials are just a few of the applications for HPAs.
 732 Phosphotungstic acid (PWA) is one of the most promising inorganic additives for PEM
 733 composites due to its high proton conductivity and excellent thermal stability.

734



735





View Article Online
DOI: 10.1039/D4MA00628C

736

737 Figure 16: Structures of (a) Keggin, (b) Lacunary Keggin [118] and Wells-Dowson [119].

738

739 HPA can be partially replaced with cesium (CsHPA) to increase its surface acidity
740 [120]. This substitution can maximise contact with the polymer matrix by decreasing
741 the solubility of salt in water while increasing its surface area. Silica-based salts
742 enhance the mechanical properties of the membrane while also improving its
743 conductivity. Metal oxides (silica, titania), functional metal oxides [121], clay [122],
744 aluminium phosphate (ALP) [123] and zeolites [124] have been used to modify the
745 SPEEK membrane as a water retainer.

746 He et al., [92] successfully incorporated β -cyclodextrin (β -CD) onto halloysite nanotubes
747 (HNTs) using polydopamine coating to make water-insoluble β -CD-DHNTs, and
748 subsequently SPEEK/ β -CD-DHNTs/HPW composite membranes were fabricated by
749 traditional solution casting. It is reported that both HPW and β -CD-DHNTs were well
750 dispersed in the SPEEK matrix because of the hydrogen bonding complexation
751 between $[\text{PW}_{12}\text{O}_{40}]^{3-}$ and β -CD. The SPEEK/ β -CD-DHNTs/HPW composite
752 membranes proton conductivity increased with the increase of HPW content (0.090 S
753 cm^{-1}), reaching the maximum of $\sim 120\%$ increase relative to that of the SPEEK
754 membrane. Cs-HPAs, were added to the SPEEK matrix by Oh et al., [93] to create
755 composite membranes. The greatest power density values (245 and 247 mW/cm^2)
756 and enhanced conductivity of approximately $2.25 \times 10^{-3} \text{ S cm}^{-1}$ at 80°C under 80%
757 RH were demonstrated by these membranes. By embedding $\text{Cs}_{2.5}\text{H}_{0.5}\text{PW}_{12}\text{O}_{40}$ on Pt
758 in a SPEEK matrix, Zhang et al., [125] and Peighambardoust et al., [94] obtained nearly
759 identical results. At 60°C and 100% relative humidity, Zhang et al., obtained a proton
760 conductivity of $5.3 \times 10^{-2} \text{ S cm}^{-1}$, while Peighambardoust et al. obtained approximately



761 $6.82 \times 10^{-2} \text{ S cm}^{-1}$, which is thought to be higher than Nafion 117. Colicchio et al. [95] also investigated SPEEK, polyethoxysiloxane (PEOS), and PWA ($\text{H}_3\text{PW}_{12}\text{O}_{40}$) with
762 20% silica (SiO_2). According to the findings, this combination's proton conductivity is
763 twice as high as pure SPEEK's at 90% relative humidity and 100 °C. Overall, the HPA-
764 modified SPEEK membranes showed higher stability and increased proton
765 conductivity values ($6.25 \times 10^{-3} \text{ S.cm}^{-1}$) when compared to the low values produced
766 by a plain SPEEK membrane ($2.21 \times 10^{-3} \text{ S.cm}^{-1}$). Therefore, the HPA/SPEEK
767 composite membranes are good candidates to replace Nafion-based membranes in
768 PEM fuel cells due to their better proton conductivity and long-term stability.

770 Dogan et al., [96] created cesium salt of tungstophosphoric acid (Cs-TPA) particles by
771 combining aqueous solutions of tungstophosphoric acid and cesium hydroxide, as well
772 as Cs-TPA particles and sulfonated (polyether ether ketone). They investigated the
773 effects of Cs-TPA on SPEEK membranes in terms of SPEEK sulfonation degrees and
774 Cs-TPA content. The composite membranes' performance was measured in terms of
775 water uptake, ion exchange capacity, proton conductivity, chemical stability, hydrolytic
776 stability, thermal stability, and methanol permeability. It was discovered that the Cs-
777 TPA particles aggregated as the degree of sulfonation of SPEEK increased from 60
778 to 70%. SPEEK (DS: 60%)/Cs-TPA membrane with 10% Cs-TPA concentration
779 reduced methanol permeability to $4.7 \times 10^{-7} \text{ cm}^2.\text{s}^{-1}$. At 80 °C and 100% RH, the
780 membrane attained an acceptable proton conductivity of $1.3 \times 10^{-1} \text{ S cm}^{-1}$. They also
781 discovered that weight loss at 900 °C increased with the inclusion of inorganic
782 particles, as expected. The addition of Cs-TPA particles to the SPEEK/Cs-TPA based
783 composite membranes increased their hydrolytic stability. The authors also discovered
784 that SPEEK60/Cs-TPA composite membranes were more hydrolytically stable than
785 SPEEK70/Cs-TPA composite membranes. SPEEK60 composite membranes had
786 reduced permeability values for methanol, water vapor, and hydrogen compared to
787 Nafion®.

788

789 **5.3 Graphene as fillers for SPEEK membrane**

790 Graphene, a two-dimensional sheet of carbon, has astounded the world with its
791 fascinating unique chemical, physical, and thermal properties, opening the door to
792 numerous applications [115]. Due to its large surface area, which is highly valued in



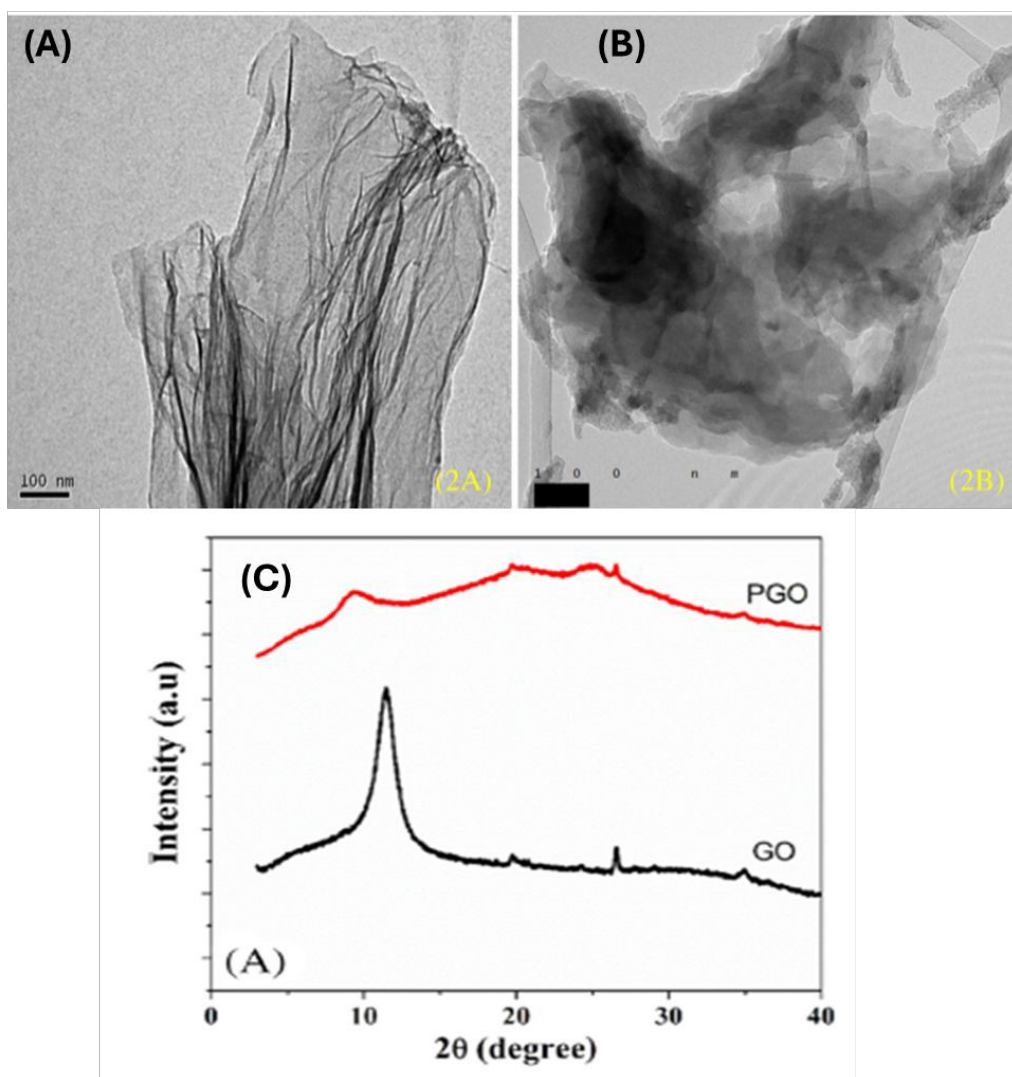
793 energy storage systems, graphene is primarily used as an electrode material in various
794 electrochemical applications. Graphene is a carbon allotrope with a honeycomb lattice
795 of sp²-hybridized two-dimensional monolayers [126]. In comparison to graphite and
796 carbon nanotubes (CNTs), graphene has a larger surface area (2629 m²/g) than CNTs
797 (1315 m²/g), and is regarded as a fundamental building block for graphitic materials
798 [127]. Graphene also has excellent electronic properties, exhibiting half integral
799 quantum Hall effect even at room temperature [128, 129]. Graphene was extracted
800 from graphite using a simple scotch tape method, and it was awarded the Nobel Prize
801 in 2010 for its discovery [130]. Since then, many scientists have shifted their research
802 focus to it, particularly in the areas of synthesis, functionalization, and application in
803 various electrochemical devices such as fuel cells, solar cells, batteries, and ultra-
804 capacitors.

805 Das et al., [131] synthesised solution-cast palladium graphite oxide-grafted amino acid
806 nanocomposites (Pd-GO-L-Tyr) in sulfonated poly(ether ether ketone) (SPEEK). The
807 composite membrane exhibited enhanced proton conductivity when compared to the
808 pristine SPEEK membrane, owing to its increased hydrophilicity, surface wettability,
809 and ion exchange capacity, which are attributed to the increased presence of hydroxy
810 and carboxyl groups. The SPEEK/Pd-GO-L-Tyr membrane's high proton conductivity
811 (2.56 mS.cm⁻¹) and low methanol crossover resulted in significantly higher selectivity
812 (5.57 × 10 S cm⁻³ s) compared to the SPEEK membrane (4.8 × 10² S cm⁻³ s⁻¹) and
813 Nafion-117 membranes (2.78 × 10³ S cm⁻³ s⁻¹). Incorporating Pd-GO-L-Tyr into the
814 SPEEK membrane matrix creates a physical barrier to prevent methanol crossover.
815 With the above-mentioned factors, the authors concluded that composite membranes
816 (Pd-GO-L-Tyr-SPEEK) are better candidates for DMFC applications, compared to the
817 standard Nafion®117 membranes. Yogarathinam et al., [97] synthesised conductive
818 polyaniline decorated graphene oxide (PANI-GO) and graphene oxide (GO), which
819 they added to a sulfonated poly(ether ether ketone) (SPEEK) nanocomposite
820 membrane to decrease methanol crossover. Surface morphology and crystallinity
821 analysis verified the formation of PANI coated GO nanostructures (Figure 17). The
822 analysis of membrane topography and morphology verified that PANI-GO and GO
823 were evenly distributed across the surface of the SPEEK membrane. With a water
824 uptake of 40% and an ion exchange capacity of 1.74 meq g⁻¹, the 0.1 wt.% PANI-GO
825 modified SPEEK nanocomposite membrane demonstrated the highest performance.



826 The nanocomposite membranes' oxidative stability was also improved. The modified
 827 SPEEK membrane with 0.1 wt.% PANI-GO had a lower methanol permeability of 4.33
 828 $\times 10^{-7} \text{ cm}^2 \cdot \text{S}^{-1}$. The presence of acidic and hydrophilic groups in PANI and GO
 829 increased the proton conductivity of the PANI-GO modified SPEEK membrane. The
 830 selectivity of the PANI-GO modified SPEEK membrane was $1.94 \times 10^4 \text{ S cm}^{-3} \text{ s}^{-1}$.
 831 PANI-GO modified SPEEK membrane was discovered to be a potential material for
 832 DMFC applications.

833



834

835 Figure 17: (A) Transmission electron microscopy (TEM) morphology of GO, (B) TEM morphology of
 836 PANI-GO nanocomposites and (C) X-ray diffractometer (XRD) patterns of GO and PANI-GO
 837 nanocomposites [97].



838 Maiti et al., [98] investigated a novel strategy for the advancement of proton exchange
839 membranes by incorporating propylsulfonic acid-functionalized graphene oxide in
840 crosslinked acid-base polymer blends and explored its fuel cells applications. The
841 molecular dynamics (MD) simulations were conducted at different PrSGO loadings for
842 the SPEEK/SPBI, XSPEEK/SPBI, and cross-linked SPEEK/SPBI composite systems.
843 After increasing the loading percentage of SPBI and PrSGO filler in the polymer matrix
844 and cross-linking the polymer composites, the glass transition temperature (T_g) was
845 increased. It was also reported that the mechanical, chemical, and thermal stability of
846 the XSPEEK/SPBI/PrSGO nanocomposite membranes increased significantly with an
847 increase in PrSGO loading, owing to the strong interfacial interaction between PrSGO
848 and the XSPEEK/SPBI matrix. The proton conductivity of the XSPEEK/SPBI/PrSGO
849 nanocomposite membrane improved significantly up to $0.17 \text{ S}\cdot\text{cm}^{-1}$ at 4 weight percent
850 PrSGO loading at 100% relative humidity (RH) and 90°C . Furthermore, at 100% RH,
851 80°C , the XSPEEK/SPBI/PrSGO nanocomposite membrane demonstrated excellent
852 fuel cell (FC) performance with a maximum power density of $0.82 \text{ W}\cdot\text{cm}^{-2}$. Due to the
853 hygroscopic nature of PRs GO, the authors observed a higher number of sulfonic acid
854 groups and excellent interaction between the acid functionalized fillers and the cross-
855 linked SPEEK/SPBI-based matrix. The membranes' overall performance and other
856 critical characteristics, including their proton conductivity, were enhanced by the
857 addition of PrSGO nanofillers to the polymer matrix.

858 **5.4 Silica as fillers for SPEEK membrane**

859 The extensive research on silica-based nanoparticles is due to their lower cost, good
860 mechanical, and water retention properties. However, due to their poor organic
861 compatibility and non-conductive properties, SiO_2 particles aggregate in the polymeric
862 matrix and reduce the conductivity of PEMs [132]. Higher silica loading in the
863 membrane results in a significant dilution effect for the membrane's ion exchangeable
864 groups [133]. As a result, as pure silica content increases, the membrane's ion
865 exchange capacity decreases [134]. However, numerous studies have been
866 conducted to improve membrane IEC by functionalizing silica filler with sulfonic group
867 derivatives. Optimal silica loading improves membrane strength [135]. Higher silica
868 content in the matrix, on the other hand, is detrimental to the mechanical properties of
869 the polymer due to increased filler-filler interaction compared to filler-polymer
870 interaction, which destroys membrane homogeneity and causes the membrane to



871 become brittle. As a result, a perfect combination of inorganic material and membrane
872 can result in nanocomposites with improved mechanical properties [136].

873 Martina et al., [99] used the solvent cast method to create Sulfonated silica (S-SiO₂)
874 nanoparticles incorporated into a blend of sulfonated poly (vinylidene fluoride-co-
875 hexafluoropropylene) (SPVdF-HFP) and sulfonated poly (ether ether ketone)
876 (SPEEK). They claimed that incorporating S-SiO₂ into SPEEK improved the polymer's
877 water uptake, IEC, and mechanical properties. At 90 °C and 100% RH, sulfonated
878 silica with an 80 wt% SPEEK-20 wt% SPVdF-HFP nanocomposite membrane
879 demonstrated maximum proton conductivity and current density of 7.9 x10⁻² S.cm⁻¹
880 and 354 mA cm⁻², respectively. The enhanced proton conductivity is attributed to the
881 presence of S-SiO₂. The hydrophilic nature promotes the ion channels and swells the
882 membrane which results in enhanced proton conductivity.

883 Meng et al., [100] investigated how amino-modified mesoporous silica nanospheres
884 affected the properties of SPEEK/phosphotungstic acid (HPW). They state that while
885 immobilising acids is an issue, adding acid proton carriers to a polymer matrix is an
886 effective method for increasing proton conductivity. They discovered that adding HPW
887 and aminated mesoporous silica nanoparticles (K-MSNs) to SPEEK enhanced
888 dimensional stability and proton conductivity. At temperature of 60 °C and 1 wt.% K-
889 MSNs loading, the composite membrane's proton conductivity was 243 mS/cm,
890 indicating that SPEEK/HPW/K-MSNs composite membranes have significant potential
891 in methanol fuel cells application. Sahin et al. produced a blending polymer consisting
892 of SPEEK, PVA, and tetraethyl orthosilicate (TEOS) [101]. The author demonstrated
893 how adding PVA could increase the number of modifiable groups, which would
894 enhance proton transport and improve oxidative and hydrolytic stability when TEOS is
895 added. This finding was supported by the author's results, which showed that the
896 SPEEK/PVA/TEOS blend outperformed the other samples (pure SPEEK, PVA, and
897 SPEEK/PVA composite) in terms of oxidative and hydrolytic stability. The addition of
898 TEOS increased hydrolytic stability while reducing the amount of –OH groups, which
899 in turn improved water resistivity. Additionally, the membrane shows better cell
900 performance values when compared to Nafion 117. The outcomes demonstrate how
901 promising these membranes are as PEMFC application candidates.



902 In another study, Li et al., [88] successfully synthesised composite membrane by
903 dispersing ionic liquid (IL) in sulfonated hollow mesoporous organosilica (sHMO) into
904 the SPEEK polymer backbone. The comparison study of various SPEEK/IL/sHMO-x
905 (where x represents: 2.5, 5.0, 7.5 and 10 wt%) composite membranes and
906 SPEEK/IL/HMO was conducted. The authors reported that SPEEK/IL-30/sHMO-7.5
907 membrane had a conductivity of 1.13 mS.cm^{-1} at $200 \text{ }^\circ\text{C}$, which is twice that of the
908 SPEEK/IL-30/HMO-7.5 (0.60 mS cm^{-1}) at same conditions. The improvement of the
909 conductivity can be attributed to the addition of sHMO might have facilitated the
910 formation of continuous network or continuous pathway with IL. The organosilica
911 sphere's surface exhibits a strong interaction between the hydroxyl group and IL,
912 leading to significant IL retention. The IL loss study revealed that adding organosilica
913 sphere significantly reduced the membrane's IL loss. The anhydrous membrane is
914 expected to be useful in PEMFCs at medium temperature conditions.

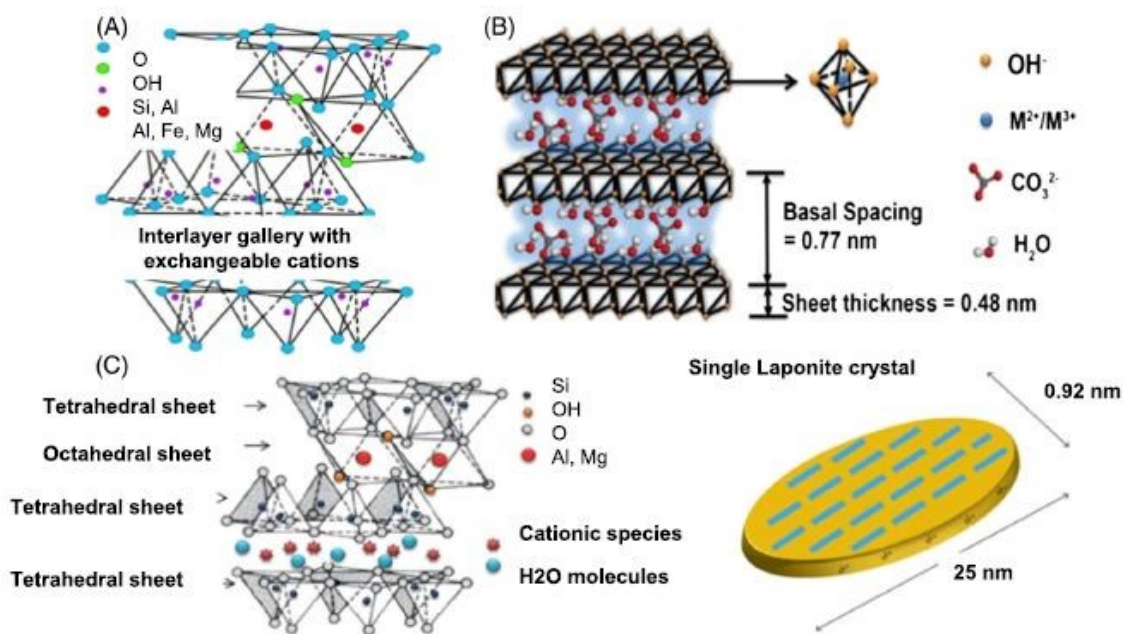
915

916 **5.5 Clay as fillers for SPEEK membrane**

917 Clay is a common nanofiller used in many different applications. Natural and synthetic
918 clays include talc, mica, layered double hydroxide (LDH), laponite (LAP), SAP, and
919 montmorillonite (MMT). The structures of laponite clay, layered double hydroxide, and
920 montmorillonite are depicted in Figure 18. Compared to mica and talc, MMT, which
921 has the chemical formula $(\text{Na,Ca})_{0.33}(\text{AlMg})_2(\text{Si}_4\text{O}_{10})(\text{OH})_2\text{nH}_2\text{O}$, has drawn a lot of
922 attention and is used as a nanofiller in many applications, including fuel cells. MMT is
923 a cation clay with a 2:1 crystal structure made up of one layer of octahedral aluminium
924 hydroxide or magnesium hydroxide sheets and two interconnected tetrahedral silicon
925 oxide sheets. LDH consists of a positively charged metal hydroxide brucite-type sheet
926 with various anions and water inside galleries to counterbalance the charge [137].
927 Apart from LDH, LAP is also a component of a synthetic clay that belongs to the 2:1
928 phyllosilicate structural group. The structure and composition of LAP, which has the
929 chemical formula $\text{Na}_{0.7}(\text{Si}_8\text{Mg}_{5.5}\text{Li}_{0.3})\text{O}_{20}(\text{OH})_4$ are similar to those of natural clay
930 hectorite minerals [138]. LAP is made up of octahedral magnesium oxide and two
931 parallel sheets of tetrahedral silica, resulting in two-dimensional layers. A single LAP
932 layer is 25 nm in diameter and 1 nm thick, with positive charges on the edges and
933 negative charges on the faces. Clay is readily available in nature and easily
934 synthesised. It has high ion-exchange capacity, chemical stability, and rheological



935 properties. Clay's thin platelet structure contributes to its high aspect ratio [139]. Due
 936 to its morphology, size, structure, and ionic nature, clay nanofiller performs
 937 exceptionally well as an electrolyte, particularly in fuel cell composite membranes.



938
 939 Figure 18: Structures of (A) montmorillonite (MMT), (B) layered double hydroxides (LDH), and (C)
 940 laponite (LAP) clays with single laponite crystal [140]

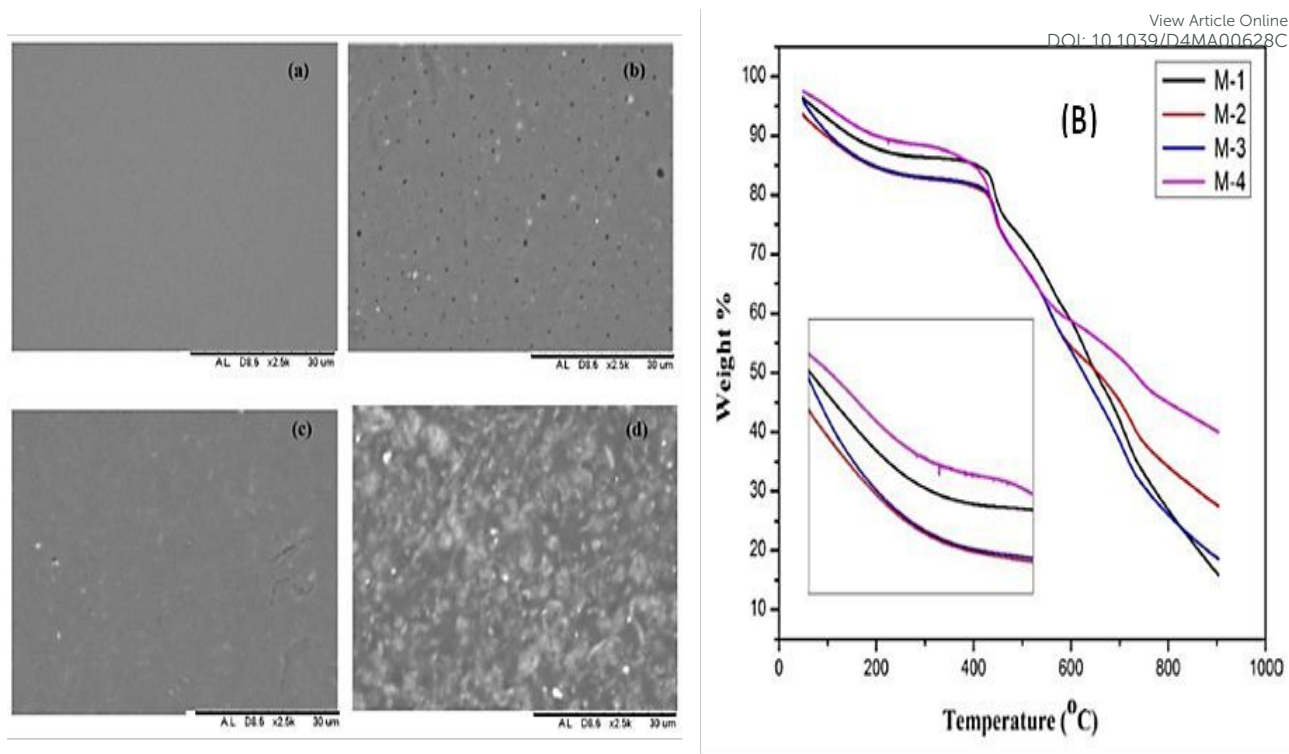
941
 942 He et al., [141] compare the performance of unmodified clays (Na⁺ montmorillonite)
 943 (IC) with that of organ modified clays (I.44P (Na⁺ montmorillonite modified by I.24TL
 944 (Na⁺montmorillonite modified by HOOC(CH₂)₁₇NH₃⁺)(HC) and (CH₃(CH₂)₁₇N(CH₃)₂⁺)
 945 (OC). When loading less than 10 wt% of HC, SPEEK/HC membrane outperforms all
 946 other types of SPEEK/clay composite membranes in terms of overall performance and
 947 achieves higher selectivity than pure SPEEK membrane. These SPEEK/HC
 948 composite membranes have been reported to have increased methanol permeability
 949 and proton conductivity. Combining the HC carboxylic acid group increased HC
 950 bonding between membrane ion groups and dispersibility due to higher proton
 951 conductivity without compromising membrane stability. For SPEEK/IC and SPEEK/OC
 952 hybrid membranes, proton conductivity simultaneously decreases with increasing filler
 953 content.



954 Kumar et al., [102] created sulfonated polyether ether ketone (SPEEK) composites
955 with of bentonite and cloisite 30B nanoclays. The enhanced glass transition
956 temperature and altered membrane morphology in the pristine SPEEK membrane
957 (Figure 19) indicated the presence of nanoclays. In comparison to the pristine
958 membrane, the addition of 0.5 weight percent of bentonite and cloisite to SPEEK
959 decreased proton conductivity and water uptake. According to the author, this could
960 be due to blocked ionic micro-structure channels caused by nano clay particles, which
961 reduce ion exchange carriers. The addition of cloisite and bentonite to SPEEK polymer
962 matrices limits the available nanometric channels for the migration of polar molecules
963 such as hydrogen ions and water. Cloisite and bentonite layers' increased rigidity
964 complicates proton transport, which accounts for the decrease in conductivity.
965 Gokulakrishnan et al., [103] synthesised membranes of functionalized graphene oxide
966 (f-GO) nanocomposites at different concentrations and halloysite nano clay using dry
967 phase inversion. The study discovered that the sulfonic acid group in SPEEK and
968 silane functionalization of GO increased the ion exchange capacity from 0.22 to 0.35
969 meq/g, which improved proton conductivity. In comparison to the pure SPEEK
970 membrane, which had proton conductivity of 0.31 mS cm^{-1} and power density of 28
971 mW cm^{-2} , the composite membrane, which contained 3 wt.% halloysite nano clay and
972 2 wt.% f-GO, maintained values of 0.47 mS cm^{-1} and 72.2 mW cm^{-2} . The 2 wt.% f-GO
973 and 3 wt.% SPEEK membranes with halloysite incorporation showed improved proton
974 conductivity; these membranes are crucial for direct methanol fuel cell (DMFC)
975 applications.

View Article Online
DOI: 10.1039/D4MA00628C





976

977 Figure 19: SEM images of various membranes: (a) SPEEK, (b) SPEEK/bentonite, (c) SPEEK/cloisite
 978 and (d)SPEEK/bentonite/cloisite, (B) TGA thermograms of SPEEK (M-1), SPEEK/cloisite (M-2),
 979 SPEEK/bentonite(M-3) and SPEEK/cloisite/bentonite (M-4) [102].

980

981 To create composite membranes with different nanofiller contents, Charradi et al.,
 982 [104] used a porous SiO₂-montmorillonite heterostructured material packed with
 983 delaminated clay particles and a synthetic Mg-Al layered double hydroxide (LDH)
 984 exchanged with sulphate anions. The addition of Mg-Al LDH and SiO₂-motmorillonite
 985 fillers to the SPEEK appears to improve water retention and thermal stability of the
 986 resulting composite electrolyte membranes. At 120°C and 100% relative humidity, Si-
 987 motmorillonite exhibited a higher proton conductivity (0.158 S.cm⁻¹) than both Mg-Al
 988 LDH and neat SPEEK (0.070 and 0.023 S.cm⁻¹, respectively). This could improve the
 989 performance of fuel cell membranes at high temperatures.

990

991 5.6 Metal Oxide as fillers for SPEEK membrane

992 Interfacial interactions between membranes and catalysts, which constitute MEA
 993 components, are critical to the proper operation of fuel cells. This interfacial interaction
 994 is closely related to the catalyst and membrane structures, as well as the method used



995 to prepare MEA [142]. Metal oxides are classified into several types, including ZrO_2 ,
996 SiO_2 , Al_2O_3 , and TiO_2 , each with its own set of properties. The conductivity of the
997 membrane protons is typically increased when a metal oxide is added as an additive
998 in composite polymers for a variety of reasons, such as the following:

- 999 1. Defects in the interface that arise when metal oxides occupy the polymer chamber
1000 and distance charge sheets are present.
- 1001 2. Metal oxides nanofillers are the predominant material in amorphous conditions
1002 because they promote proton transport and increase the free volume within the
1003 polymer matrix.
- 1004 3. Increased ion dissociation in the polymer electrolyte membrane.

1005 However, the PEM water intake and conductivity are affected by the properties and
1006 reactions of metal oxides such as strontium cerate, silica, titania, zeolite and zirconia.
1007 Because of their large aspect ratio and surface area, metal oxide nanofibers are
1008 superior to other additives for composite materials. The addition of Fe_3O_4 to PEEK,
1009 SPEEK, SPES and Nafion improved proton conductivity by promoting precise water
1010 hopping mechanisms. Furthermore, molybdenum oxide (MoO_3) has good conductivity
1011 and physicochemical properties, making it suitable for use in energy-related fields.

1012 Alumina, or aluminium oxide, is a common nanofiller in composites. Alumina has the
1013 chemical formula Al_2O_3 and can be found in a variety of minerals, including bauxite,
1014 diaspore ($Al_2O_3 \cdot H_2O$) and gibbsite ($Al_2O_3 \cdot 3H_2O$) [143, 144]. Alumina can exist in various
1015 crystalline structures, but Al_2O_3 is the most thermodynamically stable. Its large surface
1016 area and high catalytic activity make it a good nanofiller. One of the metal oxide types
1017 that is frequently utilised as a nanofiller in fuel cells is silicon oxide, or silica (SiO_2). Sol
1018 gel, microemulsion, fuming, and precipitation are a few of the techniques used to
1019 create nanoparticle silica. The hydrophilic characteristics of this metal oxide have been
1020 attributed to the development of siloxane and silanol groups on the SiO_2 surface, which
1021 is a 3D network in structure. Surface-modified SiO_2 , which comes in a range of sizes
1022 (mesopores, spheres, fibres, and rods) has been employed as a nanofiller in fuel cell
1023 membranes. The common techniques for producing the silica/polymer composite are
1024 sol-gel, in situ polymerization, and straightforward blending. The most popular
1025 technique is simple blending because it is easy to control the parameters (sonicating



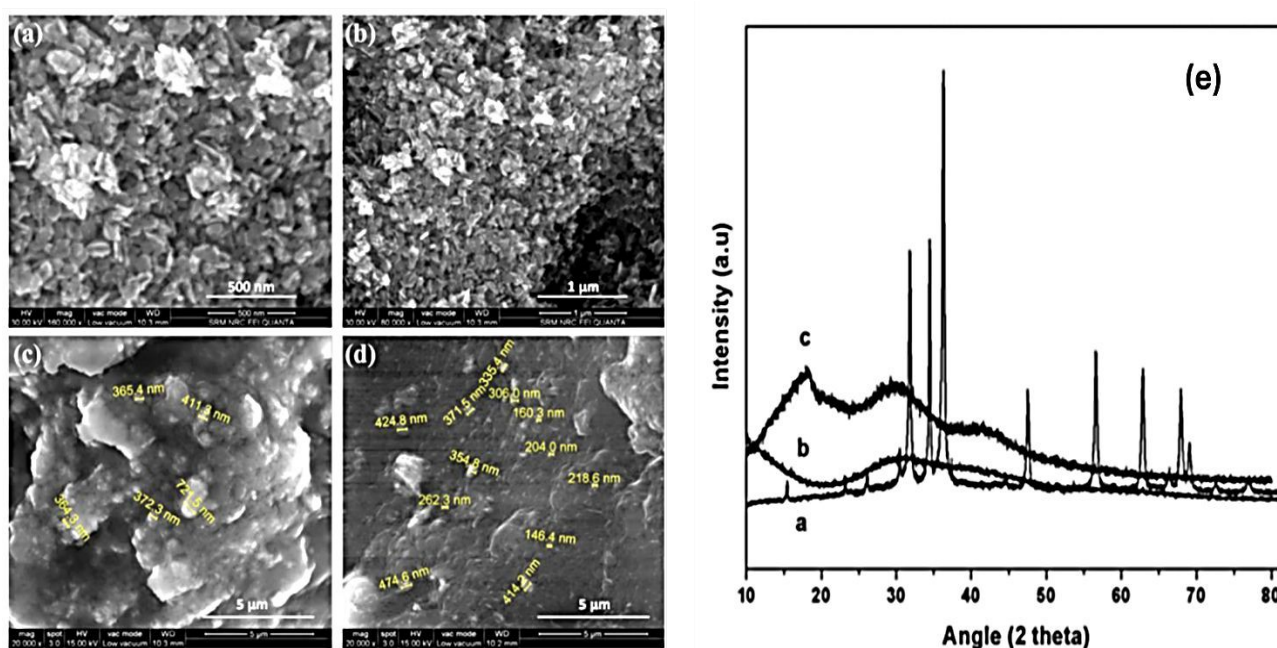
1026 time and temperature) needed to create high homogeneity of the polymer composite
1027 [145].

1028 Selvakumar et al., [105] created sulfonation PEEK membranes using the solvent
1029 casting technique of bariun zirconate (BaZrO_3). The polymer electrolyte's proton
1030 conductivity was significantly enhanced at a high weight ratio of 6 wt.% BaZrO_3 filler,
1031 with $3.12 \times 10^{-1} \text{ S.cm}^{-1}$ at 90°C . They found that the values of proton conductivity rise
1032 with increasing temperature. Proton conduction occurs because BaZrO_3 nanoparticles
1033 can dissolve protons from water in wet environments. The composite membrane
1034 exhibited current density of 280 mA cm^{-2} and power density of 183 mW cm^{-2} . The
1035 author concluded that the 94 wt% SPEEK 6 wt% BaZrO_3 polymer composite
1036 membrane is a viable option for PEM fuel cell applications. Wang et al. have effectively
1037 synthesised a sulfonated poly (ether ether ketone) (SPEEK) nanocomposite
1038 membrane through the integration of phosphotungstic acid (HPW) and aluminium
1039 doped cerium-based oxides (Al-CeZrO_4) into the SPEEK matrix [106]. The addition of
1040 Al-CeZrO_4 improved the chemical stability of SPEEK membrane while maintaining
1041 conductivity, and the addition of HPW increased proton conduction via acid-base
1042 interactions. Comparing the SPEEK/ Al-CeZrO_4 nanocomposite membrane to the
1043 SPEEK/HPW nanocomposite membrane, there was a 15.5% increase in proton
1044 conductivity. Therefore, it is believed that Al-CeZrO_4 /HPW is a useful inorganic
1045 nanofiller for enhancing the chemical stability and proton conductivity of SPEEK
1046 membranes, and more research should be done on the hybrid composite membrane.

1047 Gandhimathi et al., [107] developed sulfonation PEEK membranes by casting niobium
1048 oxide in a solvent. At a high weight ratio of 10% NBO filler, the polymer electrolyte's
1049 proton conductivity was dramatically increased to $2.9 \times 10^{-2} \text{ S.cm}^{-1}$ at 90°C , compared
1050 to $1.8 \times 10^{-2} \text{ S.cm}^{-1}$ for pure SPEEK membrane. The thermal stability of the composite
1051 membranes was also significantly enhanced by the impregnation of NBO. It was
1052 reported that SP-NBO-10 nanocomposite membrane achieved a maximum power
1053 density of 601 mW cm^{-2} , while the pristine membrane could only achieve a maximum
1054 of 497 mW cm^{-2} . The increase in the trend of current density and power density of the
1055 composite membrane may be induced by the vehicular proton transport mechanism
1056 involved in sulfonic acid-based ionomeric membrane that leads to adsorption and
1057 retention of more water molecules. Based on the electrochemical results the author
1058 concluded that the SP-NBO-10 polymer composite membrane is a feasible material



1059 for PEM fuel cell applications. Prathap et al., [108] successfully created a new set of
 1060 polymer composite membranes employing a linear sulfonated poly(ether ether ketone)
 1061 (SPEEK) polymer and zinc cobalt oxide (ZCO) as an inorganic filler, which were tested
 1062 for fuel cell applications. SPEEK was created by directly sulfonating PEEK with
 1063 concentrated sulfuric acid, then loading sufficient amounts of ZCO into it to form
 1064 polymer composites. Proton nuclear magnetic resonance investigations demonstrated
 1065 a 55% sulfonation of SPEEK, whereas XRD and morphological examinations
 1066 confirmed the successful integration of inorganic fillers into the polymer matrix, as
 1067 illustrated in Figure 20. Additionally, the authors stated that at 30°C, the pristine
 1068 SPEEK membrane had a proton conductivity of $9 \times 10^{-3} \text{ S cm}^{-1}$, while the composite
 1069 membranes loaded with 2.5 to 10 wt% of ZCO showed values in the range of 1.2×10^{-2}
 1070 $- 2 \times 10^{-2} \text{ S cm}^{-1}$. The membranes' measured ion exchange capacities fell between
 1071 1.26 and 1.46 meq g^{-1} . The composite membranes demonstrated remarkable thermal
 1072 stability up to 370°C. Thus, the membranes created in this study have the potential to
 1073 considerably contribute to the creation of new proton conducting SP-ZCO composite
 1074 membranes for use in PEM fuel cells.



1075
 1076 Figure 20: FESEM images of (a), (b) ZCO, (c) SP-ZCO-5, and (d) SP-ZCO-10, (e) XRD spectra of
 1077 SPEEK and SP-SZO nanocomposites.



1078

5.7 Metal-organic frameworks (MOFs) as fillers for SPEEK membrane

1079 Metal-organic frameworks (MOFs) are highly porous materials with tunable pore size
1080 and chemical functionality. They are created by unifying metal ions or their clusters
1081 with various organic linkers. Compared to other additives, MOFs' organic linkers
1082 provide higher loading because of their improved compatibility with the organic
1083 polymers [146, 147]. The effective manipulation of MOFs' composition and pore size
1084 can be achieved through the appropriate choice of precursors, adjustment of synthesis
1085 conditions (reagent molar ratio, temperature, etc.), or post synthetic chemical
1086 modifications. The tunable functionality of MOFs, combined with their high porosity
1087 and surface area, makes them appealing for applications involving interactions with
1088 guest species [148]. Zeolite imidazolate frameworks, or ZIFs, are a significant
1089 subclass of metal-organic frameworks (MOFs) that offer high surface area and thermal
1090 stability due to their structural similarities to zeolite and the structural diversity that
1091 MOFs provide through properties like pore size tunability and chemical functionality
1092 [149]. For small molecules like hydrogen, the tiny pores at the entrance provide a
1093 molecular sieving effect, and the large internal cavities encourage quick diffusion [150,
1094 151]. Several ZIF-polymer composite membranes containing ZIF-7, ZIF-8, ZIF-22,
1095 ZIF-90, ZIF-100, and other components have been proven to significantly improve
1096 hydrogen separation, but ZIF-8 has been successfully commercialised and widely
1097 used due to its higher stability and better resistance to acid and alkaline environments
1098 [152]. MOFs are increasingly being used in electrochemical systems for clean energy
1099 applications, such as solar cells, fuel cells, hydrogen production and storage,
1100 supercapacitors, and lithium-ion batteries. Over the last decade, the chemistry of MOF
1101 compounds has received a lot of attention for its use in many fields of material
1102 chemistry, including gas storage and separation [153], biomedical applications [154],
1103 catalysis [155], and electro-optical devices [156].
1104

1105 Zhang et al., [109] developed a (SPEEK/HPW@MIL) membrane by combining amino-
1106 modified MIL-101 (Cr) with HPW to form nano-hybrid membranes for PEMFC
1107 applications. HPW was anchored using hydrogen bonds to reduce leakage and
1108 improve overall compatibility. The SPEEK/HPW@MIL composite membrane's proton
1109 conductivity increased by 26% due to the effective anchoring effect of MIL-101(Cr)-
1110 NH₂ on HPW and the hydrogen bond network with HPW and SPEEK. Huang et al.



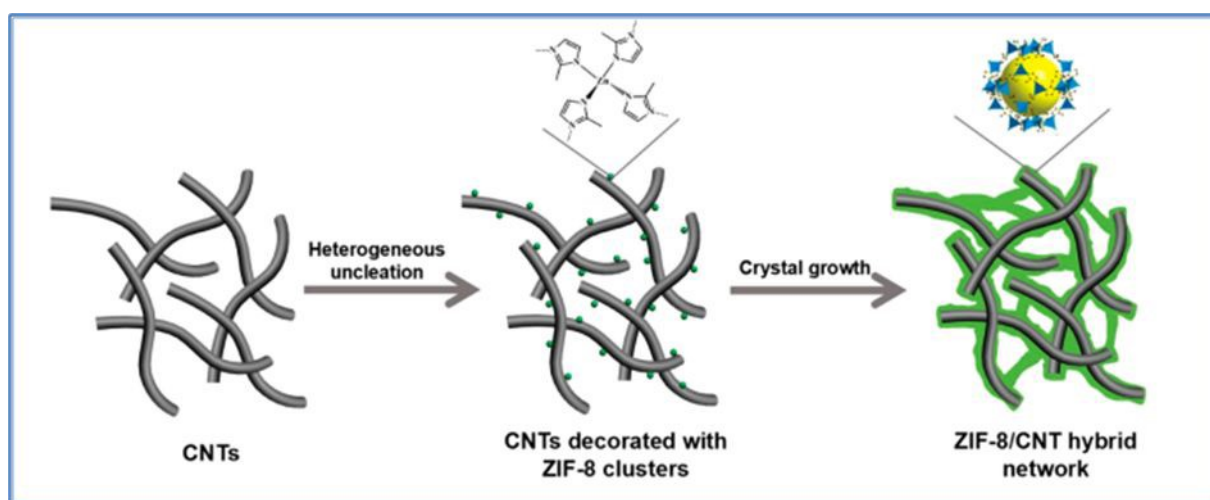
1111 created sulfonated spindle-like carbon derived from metal-organic framework, MOF-
1112 C-SO₃H, has been employed as a filler for the SPEEK membrane [110]. The obtained
1113 MOF-C-SO₃H@SPEEK membrane exhibits improved properties as a PEM for DMFCs
1114 when 3 wt.% MOF-C-SO₃H is added. They also found that the MOF-C-SO₃H@SPEEK
1115 membrane had higher proton conductivity and significantly lower methanol
1116 permeability than Nafion 115. According to their findings, the MOF-C-SO₃H@SPEEK
1117 membrane's high performance was due in large part to its specific porous and
1118 sulfonated carbon structures. The effective dispersion of MOF-C-SO₃H in the SPEEK
1119 matrix decreased the membrane's methanol permeability and swelling ratio while
1120 simultaneously enhancing proton transport and improving the membrane's proton
1121 conductivity. The authors reported a maximum power density of 83.91 mW cm⁻²,
1122 approximately 50% higher than that of Nafion 115. The superior stability of the MOF-
1123 C-SO₃H@SPEEK membrane in contrast to Nafion 115 implies that it is a viable proton
1124 exchange membrane for fuel cells.

1125 In another study, Sun et al., [111] used the solution casting method to incorporate Co-
1126 MOF-74/phosphate-4-phenylimidazole into SPEEK ternary composite membranes
1127 (Co-MOF-74/[IM₂][H₂PO₄]/SPEEK). A minor agglomeration on the surface of the Co-
1128 MOF-74/[IM₂][H₂PO₄]/ SPEEK. A ternary composite membrane with increased Co-
1129 MOF-74 contents and a gear-like structure was observed in the cross section of the
1130 prepared composite membrane using SEM. By means of hydrogen bonding, the metal
1131 organic framework (MOF) encapsulates the ionic liquid (IL) and reducing its loss,
1132 consequently enhancing the proton conductivity of the Co-MOF-74/[IM₂]
1133 [H₂PO₄]/SPEEK membrane. The authors found that using 2.5 wt.% Co-MOF-74/[IM₂]
1134 [H₂PO₄]/SPEEK resulted in a 25.96 mS·cm⁻¹ increase in proton conductivity at 120 °C,
1135 as well as a decrease in IL loss rate. Additionally, it was proposed that the Co-MOF-
1136 74/[IM₂] [H₂PO₄]/SPEEK ternary composite membrane could be used at temperatures
1137 up to 320 °C. These suggest that encapsulating IL in the MOF enhances the SPEEK
1138 membrane's thermal stability in addition to increasing its proton conductivity.

1139 Aparna et al., [112] have also fabricated Cu-MOF anchored SPEEK and SPEEK/PI
1140 composites membranes for PEMFC applications. This membrane displayed high
1141 mechanical, thermal and physiochemical properties. Cu-MOF loading at 3 wt.%
1142 resulted in maximum proton conductivity of 0.0711 S cm⁻¹ IEC value of 2.35 meq g⁻¹
1143 with a water uptake of 38.18 %. The experimental results of the prepared membranes



1144 revealed that they function as an efficient proton exchange membrane (PEM) for
 1145 PEMFCs. Sun et al., successfully synthesizes a novel two-dimensional (2D) zeolite
 1146 structure ZIF8/CNT hybrid crosslinked networks (ZCN) by in-situ growth procedure as
 1147 shown in Figure 21 [113]. The introduction of ZCN and SPEEK significantly improved
 1148 the proton conductivity and inhibited methanol permeability. The proton conductivity
 1149 of SPEEK@ZCN composite membrane was reaching 50.24 mS cm^{-1} at $120 \text{ }^\circ\text{C}$ and
 1150 30% RH, which was 11.2 times that of the recast SPEEK membrane 4.50 mS cm^{-1}
 1151 under the same conditions. Furthermore, it was discovered that the membrane's
 1152 proton conductivity was greatly enhanced by the addition of two-dimensional fillers.



1153
 1154 Figure 21: Schematic illustration of the synthesis process of ZCN through in situ growth procedure
 1155 [113]

1157 Barjola et al., [114] prepared nanocomposite membranes by mixing of 1, 3, and 5 wt%
 1158 (SPEEK-Z1, SPEEK-Z3, and SPEEK-Z5) cobalt-based zeolitic imidazolate framework
 1159 (ZIF-67) with a sulfonated poly(ether ether ketone) (SPEEK) by casting method.
 1160 Thermal stability and proton conductivity were greatly enhanced by the addition of
 1161 1wt% ZIF-67 to SPEEK. The proton conductivity of 0.014 S cm^{-1} for SPEEK-Z1
 1162 composite membrane was reported. The authors believe that a proper optimisation
 1163 process is still necessary, even though the Polymer Electrolyte Membrane Fuel Cells
 1164 (PEMFC) performance experiments showed promising results for these membranes
 1165 working at intermediate temperatures above $100 \text{ }^\circ\text{C}$.

1166



6. Conclusion and future perspectives

Without a doubt, the growing fuel cell market will provide a powerful driving force for increased research into non-fluorinated PEMs, which are less expensive and perform better than expensive Nafion® membranes. Polymers based on sulfonated poly (ether ether) ketone have the potential to be used as fuel cell electrolyte membranes. This review article examined the most current advancements in the design of various SPEEK-based electrolyte membranes for PEMFC and DMFC applications. Nevertheless, there are still certain issues with using SPEEK membranes in practical applications.: 1) SPEEKs could not achieve the excellent performance of the C-F chemical bond of PFSA membranes without any modification; 2) excessive overall swelling and low thermal stability are always caused by the higher DS of SPEEK for higher proton conductivity; 3) cross-linked SPEEK membranes formed by covalent bonds may improve dimension and chemical stability, but they will also reduce proton conductivity. Other polymers and fillers should and have been introduced into the fabrication of SPEEK membranes. As a result, one of the primary goals of future research will be to design and prepare the SPEEK membrane with proper structure in the presence of other polymers and fillers. When compared to Nafion® membranes, SPEEK's organic-inorganic composite membranes offer the best chances of superior performance. The addition of inorganic fillers may improve membrane mechanical and electrical properties, making them more suitable for fuel cell applications. However, there are still some issues that require further investigation:

- a) More hopping sites should be produced by the composite process to encourage the tendency of the proton conduction mechanisms towards the hopping mechanism, which will help to increase the methanol permeability and proton conductivity even at higher temperatures (preferably 120 °C).
- b) To strengthen the bond between filler and polymer, it's crucial to choose the right inorganic filler and modify their interface.
- c) To understand the morphology and structure of PEMs, it is important to perform dynamic simulations using mathematics and computer software. This allows for the design of modifications to SPEEK and inorganic fillers, as well as optimisation of polymer and filler combinations.

The SPEEK composite membrane has significant advantages, including low methanol crossover and high proton exchange. Proton conductivity of almost all SPEEK-related



1200 composite materials was on the order of 10^{-2} S cm⁻¹, which was adequate for them to
1201 be utilised as a membrane in a hydrogen-oxygen fuel cell. The impact of various metal
1202 oxides on the SPEEK matrix was also covered in this review, which concludes that
1203 SPEEK-based membranes are among the best polymer electrolytes for proton
1204 exchange in fuel cells. More investigation is needed to use the right inorganic particles
1205 and focus on the increase in affinity towards water-containing membranes, which
1206 increases proton conductivity. Regarding PEM development in the future, it is
1207 unrealistic to think that a single type of PEM will be able to satisfy all the needs for a
1208 larger range of applications, including stationary, mobile, and automotive fuel cell
1209 applications. Research priorities will vary depending on the application goals, but it is
1210 more important for specialists in various fields to collaborate, including physics,
1211 electrochemistry, polymers, composite materials, and simulation. As a result, we hope
1212 that this review will give a general overview of the developments surrounding SPEEK-
1213 based PEMs and offer some suggestions for the creation of high-performing non-
1214 fluorinated PEMs in the future.

1215

1216 **CRedit authorship contribution statement**

1217 **Mayetu Segale:** Conceptualization, Writing - original draft, Writing - review & editing.

1218 **Tumelo Seadira:** Conceptualization, Supervision, review & editing. **Rudzani**

1219 **Sigwadi:** Conceptualization, Supervision, review & editing. **Touhami Mokrani:**

1220 Supervision, Writing - review & editing. **Gabriel Summers:** Supervision, Writing -

1221 review & editing.

1222 **Declaration of competing interest**

1223 The authors declare that they have no known competing financial interests or personal

1224 relationships that could have appeared to influence the work reported in this paper.

1225 **Acknowledgements**

1226 We would like to acknowledge that this work has been supported in part by University

1227 of South and the National Research Foundation (NRF) of South). The opinions,

1228 findings and conclusions/recommendations expressed in this publication are those of

1229 the authors, and the NRF accepts no liability whatsoever in this regard.



1230 **7. References**

- 1231 1. Singh, P. and D. Yadav, *Link between air pollution and global climate change*, in *Global*
1232 *Climate Change*. 2021, Elsevier. p. 79-108.
- 1233 2. Al Shaikh, R., A. Al-Othman, M. Tawalbeh, A. Shamayleh, and P. Nancarrow,
1234 *Development of MXene incorporated PVDF based membranes for an enhanced*
1235 *performance in higher temperature PEM fuel cells*. *Process Safety and Environmental*
1236 *Protection*, 2024. **189**: p. 985-994.
- 1237 3. Al-Othman, A., M. Tawalbeh, A. Ka'aki, I. Shomope, and M.F. Hassan, *Novel zirconium*
1238 *phosphate/MXene/ionic liquid membranes for PEM fuel cells operating up to 145° C*.
1239 *Process Safety and Environmental Protection*, 2024. **189**: p. 1368-1378.
- 1240 4. Ali, A.A., A. Al-Othman, and M. Tawalbeh, *Exploring natural polymers for the*
1241 *development of proton exchange membranes in fuel cells*. *Process Safety and*
1242 *Environmental Protection*, 2024. **189**: p. 1379-1401.
- 1243 5. Nimir, W., A. Al-Othman, and M. Tawalbeh, *Unveiling zirconium phytate-*
1244 *heteropolyacids-ionic liquids membranes for PEM fuel cells applications up to 150° C*.
1245 *International Journal of Hydrogen Energy*, 2024.
- 1246 6. Abdelkareem, M.A., K. Elsaid, T. Wilberforce, M. Kamil, E.T. Sayed, and A. Olabi,
1247 *Environmental aspects of fuel cells: A review*. *Science of The Total Environment*, 2021.
1248 **752**: p. 141803.
- 1249 7. Nazir, H., N. Muthuswamy, C. Louis, S. Jose, J. Prakash, M.E. Buan, C. Flox, S.
1250 Chavan, X. Shi, and P. Kauranen, *Is the H2 economy realizable in the foreseeable*
1251 *future? Part III: H2 usage technologies, applications, and challenges and opportunities*.
1252 *International journal of hydrogen energy*, 2020. **45**(53): p. 28217-28239.
- 1253 8. Mohammed, H., A. Al-Othman, P. Nancarrow, M. Tawalbeh, and M.E.H. Assad, *Direct*
1254 *hydrocarbon fuel cells: A promising technology for improving energy efficiency*.
1255 *Energy*, 2019. **172**: p. 207-219.
- 1256 9. Suter, T.A., K. Smith, J. Hack, L. Rasha, Z. Rana, G.M.A. Angel, P.R. Shearing, T.S.
1257 Miller, and D.J. Brett, *Engineering Catalyst Layers for Next-Generation Polymer*
1258 *Electrolyte Fuel Cells: A Review of Design, Materials, and Methods*. *Advanced Energy*
1259 *Materials*, 2021. **11**(37): p. 2101025.
- 1260 10. Wang, Y., K.S. Chen, J. Mishler, S.C. Cho, and X.C. Adroher, *A review of polymer*
1261 *electrolyte membrane fuel cells: technology, applications, and needs on fundamental*
1262 *research*. *Applied Energy*, 2011. **88**(4): p. 981-1007.
- 1263 11. Zhang, H. and P.K. Shen, *Recent development of polymer electrolyte membranes for*
1264 *fuel cells*. *Chemical reviews*, 2012. **112**(5): p. 2780-2832.
- 1265 12. Xiao, F., Y.C. Wang, Z.P. Wu, G. Chen, F. Yang, S. Zhu, K. Siddharth, Z. Kong, A. Lu,
1266 and J.C. Li, *Recent advances in electrocatalysts for proton exchange membrane fuel*
1267 *cells and alkaline membrane fuel cells*. *Advanced Materials*, 2021. **33**(50): p. 2006292.
- 1268 13. Gao, X., J. Chen, R. Xu, Z. Zhen, X. Zeng, X. Chen, and L. Cui, *Research progress*
1269 *and prospect of the materials of bipolar plates for proton exchange membrane fuel*
1270 *cells (PEMFCs)*. *International Journal of Hydrogen Energy*, 2023.
- 1271 14. Shabani, B., M. Hafttananian, S. Khamani, A. Ramiar, and A. Ranjbar, *Poisoning of*
1272 *proton exchange membrane fuel cells by contaminants and impurities: Review of*
1273 *mechanisms, effects, and mitigation strategies*. *Journal of Power Sources*, 2019. **427**:
1274 p. 21-48.
- 1275 15. Ogungbemi, E., O. Ijaodola, F. Khatib, T. Wilberforce, Z. El Hassan, J. Thompson, M.
1276 Ramadan, and A. Olabi, *Fuel cell membranes—Pros and cons*. *Energy*, 2019. **172**: p.
1277 155-172.
- 1278 16. Kim, D.J., M.J. Jo, and S.Y. Nam, *A review of polymer–nanocomposite electrolyte*
1279 *membranes for fuel cell application*. *Journal of Industrial and Engineering Chemistry*,
1280 2015. **21**: p. 36-52.
- 1281 17. Gagliardi, G.G., A. Ibrahim, D. Borello, and A. El-Kharouf, *Composite polymers*
1282 *development and application for polymer electrolyte membrane technologies—A*
1283 *review*. *Molecules*, 2020. **25**(7): p. 1712.



- 1284 18. Walkowiak-Kulikowska, J., J. Wolska, and H. Koroniak, *10. Polymers application in proton exchange membranes for fuel cells (PEMFCs)*. Polymer Engineering, 2017: p. 293-348. View Article Online
DOI: 10.1039/D4MA00628C
- 1285
- 1286
- 1287 19. Park, C.H., C.H. Lee, M.D. Guiver, and Y.M. Lee, *Sulfonated hydrocarbon membranes for medium-temperature and low-humidity proton exchange membrane fuel cells (PEMFCs)*. Progress in Polymer Science, 2011. **36**(11): p. 1443-1498.
- 1288
- 1289
- 1290 20. Ghita, O., E. James, R. Trimble, and K.E. Evans, *Physico-chemical behaviour of poly (ether ketone)(PEK) in high temperature laser sintering (HT-LS)*. Journal of Materials Processing Technology, 2014. **214**(4): p. 969-978.
- 1291
- 1292
- 1293 21. Huang, Z., J. Liu, Y. Liu, Y. Xu, R. Li, H. Hong, L. Shen, H. Lin, and B.-Q. Liao, *Enhanced permeability and antifouling performance of polyether sulfone (PES) membrane via elevating magnetic Ni@ MXene nanoparticles to upper layer in phase inversion process*. Journal of Membrane Science, 2021. **623**: p. 119080.
- 1294
- 1295
- 1296
- 1297 22. Luo, H., G. Vaivars, and M. Mathe, *Double cross-linked polyetheretherketone proton exchange membrane for fuel cell*. international journal of hydrogen energy, 2012. **37**(7): p. 6148-6152.
- 1298
- 1299
- 1300 23. Kausar, A., *Progression from polyimide to polyimide composite in proton-exchange membrane fuel cell: a review*. Polymer-Plastics Technology and Engineering, 2017. **56**(13): p. 1375-1390.
- 1301
- 1302
- 1303 24. Gil, M., X. Ji, X. Li, H. Na, J.E. Hampsey, and Y. Lu, *Direct synthesis of sulfonated aromatic poly (ether ether ketone) proton exchange membranes for fuel cell applications*. Journal of membrane science, 2004. **234**(1-2): p. 75-81.
- 1304
- 1305
- 1306 25. Mahimai, B.M., G. Sivasubramanian, K. Sekar, D. Kannaiyan, and P. Deivanayagam, *Sulfonated poly (ether ether ketone): efficient ion-exchange polymer electrolytes for fuel cell applications—a versatile review*. Materials Advances, 2022. **3**(15): p. 6085-6095.
- 1307
- 1308
- 1309
- 1310 26. Govinna, N.D., T. Keller, C. Schick, and P. Cebe, *Melt-electrospinning of poly (ether ether ketone) fibers to avoid sulfonation*. Polymer, 2019. **171**: p. 50-57.
- 1311
- 1312 27. Sarirchi, S., S. Rowshanzamir, and F. Mehri, *Simultaneous improvement of ionic conductivity and oxidative stability of sulfonated poly (ether ether ketone) nanocomposite proton exchange membrane for fuel cell application*. International Journal of Energy Research, 2020. **44**(4): p. 2783-2800.
- 1313
- 1314
- 1315
- 1316 28. RS, R.R., W. Rashmi, M. Khalid, W. Wong, and J. Priyanka, *Recent progress in the development of aromatic polymer-based proton exchange membranes for fuel cell applications*. Polymers, 2020. **12**(5): p. 1061.
- 1317
- 1318
- 1319 29. Beyraghi, F., S.H. Mirfarsi, S. Rowshanzamir, A. Karimi, and M.J. Parnian, *Optimal thermal treatment conditions for durability improvement of highly sulfonated poly (ether ether ketone) membrane for polymer electrolyte fuel cell applications*. international journal of hydrogen energy, 2020. **45**(24): p. 13441-13458.
- 1320
- 1321
- 1322
- 1323 30. Ren, S., H. Lei, L. Wang, Q. Bu, S. Chen, and J. Wu, *Thermal behaviour and kinetic study for woody biomass torrefaction and torrefied biomass pyrolysis by TGA*. Biosystems engineering, 2013. **116**(4): p. 420-426.
- 1324
- 1325
- 1326 31. Zakaria, Z., N. Shaari, S.K. Kamarudin, R. Bahru, and M.T. Musa, *A review of progressive advanced polymer nanohybrid membrane in fuel cell application*. International Journal of Energy Research, 2020. **44**(11): p. 8255-8295.
- 1327
- 1328
- 1329 32. Gilois, B., F. Goujon, A. Fleury, A. Soldera, and A. Ghoufi, *Water nano-diffusion through the Nafion fuel cell membrane*. Journal of Membrane Science, 2020. **602**: p. 117958.
- 1330
- 1331
- 1332 33. Wang, G., Z. Liu, C. Liu, and W. Chen, *Molecular Study of Nonequilibrium Transport Mechanism for Proton and Water in Porous Proton Exchange Membranes*. International Journal of Energy Research, 2023. **2023**.
- 1333
- 1334
- 1335 34. Haider, R., Y. Wen, Z.-F. Ma, D.P. Wilkinson, L. Zhang, X. Yuan, S. Song, and J. Zhang, *High temperature proton exchange membrane fuel cells: progress in advanced materials and key technologies*. Chemical Society Reviews, 2021. **50**(2): p. 1138-1187.
- 1336
- 1337
- 1338



- 1339 35. Dong, X., D. Lu, T.A. Harris, and I.C. Escobar, *Polymers and solvents used in membrane fabrication: a review focusing on sustainable membrane development*. Membranes, 2021. **11**(5): p. 309. View Article Online
DOI: 10.1059/D4MA00628C
- 1340
- 1341
- 1342 36. Mukeba, K.M., *Step-growth polymerization of perfluoro-vinyl ether, -cycloalkenes, and acyclic alkenes with bisphenols containing variable polycyclic aromatic cores*. 2022: Mississippi State University.
- 1343
- 1344
- 1345 37. Bossion, A., K.V. Heifferon, L. Meabe, N. Zivic, D. Taton, J.L. Hedrick, T.E. Long, and H. Sardon, *Opportunities for organocatalysis in polymer synthesis via step-growth methods*. Progress in Polymer Science, 2019. **90**: p. 164-210.
- 1346
- 1347
- 1348 38. Yang, Y., Y. Wang, M. Zhu, J. Zhao, D. Cai, and H. Cao, *Valorization of lignin for renewable non-isocyanate polyurethanes: a state-of-the-art review*. Materials Today Sustainability, 2023. **22**: p. 100367.
- 1349
- 1350
- 1351 39. Nguyen, M.D.T., S. Yang, and D. Kim, *Pendant dual sulfonated poly (arylene ether ketone) proton exchange membranes for fuel cell application*. Journal of Power Sources, 2016. **328**: p. 355-363.
- 1352
- 1353
- 1354 40. Fulcrand, H., L. Rouméas, G. Billerach, C. Aouf, and E. Dubreucq, *Advances in Bio-based thermosetting polymers*. Recent Advances in Polyphenol Research, 2019. **6**: p. 285-334.
- 1355
- 1356
- 1357 41. Sun, Y., S. Zhou, G. Qin, J. Guo, Q. Zhang, S. Li, and S. Zhang, *A chemical-induced crystallization strategy to fabricate poly (ether ether ketone) asymmetric membranes for organic solvent nanofiltration*. Journal of Membrane Science, 2021. **620**: p. 118899.
- 1358
- 1359
- 1360 42. Xu, M., H. Xue, Q. Wang, and L. Jia, *Sulfonated poly (arylene ether) s based proton exchange membranes for fuel cells*. International Journal of Hydrogen Energy, 2021. **46**(62): p. 31727-31753.
- 1361
- 1362
- 1363 43. Nor, N.A.M., M.A. Mohamed, and J. Jaafar, *Modified sulfonated polyphenylsulfone proton exchange membrane with enhanced fuel cell performance: A review*. Journal of Industrial and Engineering Chemistry, 2022.
- 1364
- 1365
- 1366 44. Khomein, P., W. Ketelaars, T. Lap, and G. Liu, *Sulfonated aromatic polymer as a future proton exchange membrane: A review of sulfonation and crosslinking methods*. Renewable and Sustainable Energy Reviews, 2021. **137**: p. 110471.
- 1367
- 1368
- 1369 45. Harun, N.A.M., N. Shaari, and N.F.H. Nik Zaiman, *A review of alternative polymer electrolyte membrane for fuel cell application based on sulfonated poly (ether ether ketone)*. International Journal of Energy Research, 2021. **45**(14): p. 19671-19708.
- 1370
- 1371
- 1372 46. Sayed Daud, S.N.S., M.N.A. Mohd Norddin, J. Jaafar, and R. Sudirman, *High degree sulfonated poly (ether ether ketone) blend with polyvinylidene fluoride as a potential proton-conducting membrane fuel cell*. High Performance Polymers, 2020. **32**(1): p. 103-115.
- 1373
- 1374
- 1375
- 1376 47. Muthu Lakshmi, R., V. Choudhary, and I. Varma, *Sulphonated poly (ether ether ketone): Synthesis and characterisation*. Journal of materials science, 2005. **40**: p. 629-636.
- 1377
- 1378
- 1379 48. Tsai, S., *Introduction to composite materials*. 2018: Routledge.
- 1380
- 1381 49. Li, Z., R. Yu, C. Liu, J. Zheng, J. Guo, T.A. Sherazi, S. Li, and S. Zhang, *Preparation and characterization of side-chain poly (aryl ether ketone) anion exchange membranes by superacid-catalyzed reaction*. Polymer, 2021. **222**: p. 123639.
- 1382
- 1383 50. Wong, C.Y., W.Y. Wong, K.S. Loh, W.R.W. Daud, K.L. Lim, M. Khalid, and R. Walvekar, *Development of poly (vinyl alcohol)-based polymers as proton exchange membranes and challenges in fuel cell application: a review*. Polymer reviews, 2020. **60**(1): p. 171-202.
- 1384
- 1385
- 1386
- 1387 51. Xiang, Z., H. Liu, P. Deng, M. Liu, Y. Yin, and X. Ge, *The effect of irradiation on morphology and properties of the PET/HDPE blends with trimethylol propane trimethacrylate (TMPTA)*. Polymer bulletin, 2009. **63**: p. 587-597.
- 1388
- 1389
- 1390 52. Xiaomin, G., L. Yonghua, and L. Jinlong, *Review on modification of sulfonated poly (- ether-ether-ketone) membranes used as proton exchange membranes*. Materials Science, 2015. **21**(4): p. 574-582.
- 1391
- 1392



- 1393 53. Hayes, S., C. Boote, C.S. Kamma-Lorger, M.S. Rajan, J. Harris, E. Dooley, N. Hawksorth, J. Hiller, N.J. Terill, and F. Hafezi, *Riboflavin/UVA collagen cross-linking-induced changes in normal and keratoconus corneal stroma*. PloS one, 2011. **6**(8): p. e22405. View Article Online
DOI: 10.1098/DMAA00628C
- 1394
- 1395
- 1396
- 1397 54. Gao, Y., K. Peng, and S. Mitragotri, *Covalently Crosslinked hydrogels via step-growth reactions: crosslinking chemistries, polymers, and clinical impact*. Advanced Materials, 2021. **33**(25): p. 2006362.
- 1398
- 1399
- 1400 55. Wu, S., J. Liang, Y. Shi, M. Huang, X. Bi, Z. Wang, and J. Jin, *Design of interchain hydrogen bond in polyimide membrane for improved gas selectivity and membrane stability*. Journal of Membrane Science, 2021. **618**: p. 118659.
- 1401
- 1402
- 1403 56. Ramly, N., N. Aini, N. Sahli, S. Aminuddin, M. Yahya, and A. Ali, *Dielectric behaviour of UV-crosslinked sulfonated poly (ether ether ketone) with methyl cellulose (SPEEK-MC) as proton exchange membrane*. International Journal of Hydrogen Energy, 2017. **42**(14): p. 9284-9292.
- 1404
- 1405
- 1406
- 1407 57. Teruel-Juanes, R., B. Pascual-Jose, C. del Río, O. García, and A. Ribes-Greus, *Dielectric analysis of photocrosslinked and post-sulfonated styrene-ethylene-butylene-styrene block copolymer based membranes*. Reactive and Functional Polymers, 2020. **155**: p. 104715.
- 1408
- 1409
- 1410
- 1411 58. Meng, N., F. Lian, and G. Cui, *Macromolecular design of lithium conductive polymer as electrolyte for solid-state lithium batteries*. Small, 2021. **17**(3): p. 2005762.
- 1412
- 1413 59. Kumari, M., H.S. Sodaye, D. Sen, and R.C. Bindal, *Properties and morphology studies of proton exchange membranes based on cross-linked sulfonated poly (ether ether ketone) for electrochemical application: effect of cross-linker chain length*. Solid State Ionics, 2018. **316**: p. 75-84.
- 1414
- 1415
- 1416
- 1417 60. Gupta, D. and V. Choudhary, *Studies on novel heat treated sulfonated poly (ether ether ketone)[SPEEK]/diol membranes for fuel cell applications*. international journal of hydrogen energy, 2011. **36**(14): p. 8525-8535.
- 1418
- 1419
- 1420 61. Ajitha, A. and S. Thomas, *Introduction: Polymer blends, thermodynamics, miscibility, phase separation, and compatibilization*, in *Compatibilization of polymer blends*. 2020, Elsevier. p. 1-29.
- 1421
- 1422
- 1423 62. Liang, J., J. Ge, K. Wu, Q. Zhang, J. Wang, and Z. Ye, *Sulfonated polyaryletherketone with pendant benzimidazole groups for proton exchange membranes*. Journal of Membrane Science, 2020. **597**: p. 117626.
- 1424
- 1425
- 1426 63. Simari, C., C.L. Vecchio, V. Baglio, and I. Nicotera, *Sulfonated polyethersulfone/polyetheretherketone blend as high performing and cost-effective electrolyte membrane for direct methanol fuel cells*. Renewable Energy, 2020. **159**: p. 336-345.
- 1427
- 1428
- 1429
- 1430 64. Raja, K., M. Raja Pugalenti, and M. Ramesh Prabhu, *Investigation on the sulfonated poly (ether ether ketone)/poly (amide-imide)/barium cerate-based nanocomposite membrane for proton exchange membrane fuel cells*. International Journal of Energy Research, 2021. **45**(6): p. 8564-8576.
- 1431
- 1432
- 1433
- 1434 65. Li, C., Z. Yang, X. Liu, Y. Zhang, J. Dong, Q. Zhang, and H. Cheng, *Enhanced performance of sulfonated poly (ether ether ketone) membranes by blending fully aromatic polyamide for practical application in direct methanol fuel cells (DMFCs)*. international journal of hydrogen energy, 2017. **42**(47): p. 28567-28577.
- 1435
- 1436
- 1437
- 1438 66. Haragirimana, A., P.B. Ingabire, Y. Liu, N. Li, Z. Hu, and S. Chen, *An effective strategy to enhance the performance of the proton exchange membranes based on sulfonated poly (ether ether ketone) s*. International Journal of Hydrogen Energy, 2020. **45**(16): p. 10017-10029.
- 1439
- 1440
- 1441
- 1442 67. Shang, Z., R. Wycisk, and P. Pintauro, *Electrospun composite proton-exchange and anion-exchange membranes for fuel cells*. Energies, 2021. **14**(20): p. 6709.
- 1443
- 1444 68. Qian, X., M. Ostwal, A. Asatekin, G.M. Geise, Z.P. Smith, W.A. Phillip, R.P. Lively, and J.R. McCutcheon, *A critical review and commentary on recent progress of additive manufacturing and its impact on membrane technology*. Journal of Membrane Science, 2022. **645**: p. 120041.
- 1445
- 1446
- 1447



- 1448 69. Nayak, J.K., U. Shankar, and K. Samal, *Fabrication and development of* New Article Online
DOI: 10.1039/D4MA00628C
SPEEK/PVdF-HFP/SiO₂ proton exchange membrane for microbial fuel cell
1449 *application*. Chemical Engineering Journal Advances, 2023. **14**: p. 100459.
1450
1451 70. Çalı, A., A. Şahin, and A. Irfan, *Experimental Investigation of boron phosphate*
1452 *Incorporated speak/pvdf blend membrane for proton exchange membrane fuel cells*.
1453 International Journal of Hydrogen Energy, 2022. **47**(95): p. 40476-40490.
1454 71. Wang, D. and C.J. Cornelius, *Ionomer thermodynamic interrelationships associated*
1455 *with wettability, surface energy, swelling, and water transport*. European Polymer
1456 Journal, 2016. **85**: p. 126-138.
1457 72. Liu, Q., X. Li, S. Zhang, Z. Wang, Y. Chen, S. Zhou, C. Wang, K. Wu, J. Liu, and Q.
1458 Mao, *Novel sulfonated N-heterocyclic poly (aryl ether ketone ketone) s with pendant*
1459 *phenyl groups for proton exchange membrane performing enhanced oxidative stability*
1460 *and excellent fuel cell properties*. Journal of Membrane Science, 2022. **641**: p. 119926.
1461 73. Zhao, G., L. Shi, M. Zhang, B. Cheng, G. Yang, and X. Zhuang, *Self-assembly of*
1462 *metal-organic framework onto nanofibrous mats to enhance proton conductivity for*
1463 *proton exchange membrane*. International Journal of Hydrogen Energy, 2021. **46**(73):
1464 p. 36415-36423.
1465 74. da Trindade, L., L. Zanchet, R. Dreon, J. Souza, M. Assis, E. Longo, E. Martini, A.
1466 Chiquito, and F. Pontes, *Microwave-assisted solvothermal preparation of Zr-BDC for*
1467 *modification of proton exchange membranes made of SPEEK/PBI blends*. Journal of
1468 Materials Science, 2020. **55**: p. 14938-14952.
1469 75. Daud, S.N.S.S., M.M. Norddin, J. Jaafar, R. Sudirman, M. Othman, and A. Ismail,
1470 *Highly sulfonated poly (ether ether ketone) blend with hydrophobic polyether sulfone*
1471 *as an alternative electrolyte for proton exchange membrane fuel cell*. Arabian Journal
1472 for Science and Engineering, 2021. **46**: p. 6189-6205.
1473 76. Wei, P., Y. Sui, X. Li, Q. Liu, B. Zhu, C. Cong, X. Meng, and Q. Zhou, *Sandwich-*
1474 *structure PI/SPEEK/PI proton exchange membrane developed for achieving the high*
1475 *durability on excellent proton conductivity and stability*. Journal of Membrane Science,
1476 2022. **644**: p. 120116.
1477 77. Chu, F., X. Chu, T. Lv, Z. Chen, Y. Ren, S. Zhang, N. Yuan, B. Lin, and J. Ding,
1478 *Amphoteric membranes based on sulfonated polyether ether ketone and*
1479 *imidazolium-functionalized polyphenylene oxide for vanadium redox flow battery*
1480 *applications*. ChemElectroChem, 2019. **6**(19): p. 5041-5050.
1481 78. Yang, X., H. Zhu, F. Jiang, and X. Zhou, *Notably enhanced proton conductivity by*
1482 *thermally-induced phase-separation transition of Nafion/Poly (vinylidene fluoride)*
1483 *blend membranes*. Journal of Power Sources, 2020. **473**: p. 228586.
1484 79. Liu, G., W.-C. Tsen, S.-C. Jang, F. Hu, F. Zhong, H. Liu, G. Wang, S. Wen, G. Zheng,
1485 and C. Gong, *Mechanically robust and highly methanol-resistant sulfonated poly (ether*
1486 *ether ketone)/poly (vinylidene fluoride) nanofiber composite membranes for direct*
1487 *methanol fuel cells*. Journal of Membrane Science, 2019. **591**: p. 117321.
1488 80. Chamakh, M. and A.I. Ayesh, *Production and investigation of flexible nanofibers of*
1489 *sPEEK/PVP loaded with RuO₂ nanoparticles*. Materials & Design, 2021. **204**: p.
1490 109678.
1491 81. Purnama, H., M. Mujiburohman, M. Hakim, and N. Hidayati. *Preparation and*
1492 *Characterisation of Composite Sulfonated Polyether Ether Ketone for Direct Methanol*
1493 *Fuel Cells*. in *Journal of Physics: Conference Series*. 2019. IOP Publishing.
1494 82. Abu-Thabit, N.Y., S.A. Ali, S.J. Zaidi, and K. Mezghani, *Novel sulfonated poly (ether*
1495 *ether ketone)/phosphonated polysulfone polymer blends for proton conducting*
1496 *membranes*. Journal of Materials Research, 2012. **27**(15): p. 1958-1968.
1497 83. Sultan, A., J.K. Adewole, A. Al-Ahmed, M. Nazal, and S.J. Zaidi, *Preparation and*
1498 *performance evaluation of speak/polyaniline composite membrane for direct methanol*
1499 *fuel cell*. International Polymer Processing, 2017. **32**(1): p. 41-49.
1500 84. Han, M., G. Zhang, M. Li, S. Wang, Z. Liu, H. Li, Y. Zhang, D. Xu, J. Wang, and J. Ni,
1501 *Sulfonated poly (ether ether ketone)/polybenzimidazole oligomer/epoxy resin*



- 1502 *composite membranes in situ polymerization for direct methanol fuel cell usages*.
 1503 Journal of Power Sources, 2011. **196**(23): p. 9916-9923.
- 1504 85. Hidayati, N., T. Harmoko, M. Mujiburohman, and H. Purnama. *Characterization of*
 1505 *sPEEK/chitosan membrane for the direct methanol fuel cell*. in *AIP Conference*
 1506 *Proceedings*. 2019. AIP Publishing.
- 1507 86. Sun, X., S.C. Simonsen, T. Norby, and A. Chatzidakis, *Composite membranes for high*
 1508 *temperature PEM fuel cells and electrolyzers: a critical review*. Membranes, 2019. **9**(7):
 1509 p. 83.
- 1510 87. Liu, G., W.-C. Tsen, S.-C. Jang, F. Hu, F. Zhong, B. Zhang, J. Wang, H. Liu, G. Wang,
 1511 and S. Wen, *Composite membranes from quaternized chitosan reinforced with*
 1512 *surface-functionalized PVDF electrospun nanofibers for alkaline direct methanol fuel*
 1513 *cells*. Journal of Membrane Science, 2020. **611**: p. 118242.
- 1514 88. Li, Z., Z. Guan, C. Wang, B. Quan, and L. Zhao, *Addition of modified hollow*
 1515 *mesoporous organosilica in anhydrous SPEEK/IL composite membrane enhances its*
 1516 *proton conductivity*. Journal of Membrane Science, 2021. **620**: p. 118897.
- 1517 89. Sivasubramanian, G., K. Hariharasubramanian, P. Deivanayagam, and J.
 1518 Ramaswamy, *High-performance SPEEK/SWCNT/fly ash polymer electrolyte*
 1519 *nanocomposite membranes for fuel cell applications*. Polymer Journal, 2017. **49**(10):
 1520 p. 703-709.
- 1521 90. Gahlot, S. and V. Kulshrestha, *Dramatic improvement in water retention and proton*
 1522 *conductivity in electrically aligned functionalized CNT/SPEEK nanohybrid PEM*. ACS
 1523 Applied Materials & Interfaces, 2015. **7**(1): p. 264-272.
- 1524 91. Di, Y., W. Yang, X. Li, Z. Zhao, M. Wang, and J. Dai, *Preparation and characterization*
 1525 *of continuous carbon nanofiber-supported SPEEK composite membranes for fuel cell*
 1526 *application*. RSC Advances, 2014. **4**(94): p. 52001-52007.
- 1527 92. He, S., Y. Ai, W. Dai, S. Zhai, H. Song, and J. Lin, *Composite membranes anchoring*
 1528 *phosphotungstic acid by β -cyclodextrins modified halloysite nanotubes*. Polymer
 1529 Testing, 2021. **100**: p. 107246.
- 1530 93. Oh, S., T. Yoshida, G. Kawamura, H. Muto, M. Sakai, and A. Matsuda, *Proton*
 1531 *conductivity and fuel cell property of composite electrolyte consisting of Cs-substituted*
 1532 *heteropoly acids and sulfonated poly (ether-ether ketone)*. Journal of Power Sources,
 1533 2010. **195**(18): p. 5822-5828.
- 1534 94. Peighambardoust, S., S. Rowshanzamir, M. Hosseini, and M. Yazdanpour, *Self-*
 1535 *humidifying nanocomposite membranes based on sulfonated poly (ether ether ketone)*
 1536 *and heteropolyacid supported Pt catalyst for fuel cells*. International journal of
 1537 hydrogen energy, 2011. **36**(17): p. 10940-10957.
- 1538 95. Colicchio, I., F. Wen, H. Keul, U. Simon, and M. Moeller, *Sulfonated poly (ether ether*
 1539 *ketone)-silica membranes doped with phosphotungstic acid. Morphology and proton*
 1540 *conductivity*. Journal of Membrane Science, 2009. **326**(1): p. 45-57.
- 1541 96. Doğan, H., T.Y. Inan, E. Unveren, and M. Kaya, *Effect of cesium salt of*
 1542 *tungstophosphoric acid (Cs-TPA) on the properties of sulfonated polyether ether*
 1543 *ketone (SPEEK) composite membranes for fuel cell applications*. international journal
 1544 of hydrogen energy, 2010. **35**(15): p. 7784-7795.
- 1545 97. Yogarathinam, L.T., J. Jaafar, A.F. Ismail, P.S. Goh, M.H. Bin Mohamed, M.F. Radzi
 1546 Hanifah, A. Gangasalam, and J. Peter, *Polyaniline decorated graphene oxide on*
 1547 *sulfonated poly (ether ether ketone) membrane for direct methanol fuel cells*
 1548 *application*. Polymers for Advanced Technologies, 2022. **33**(1): p. 66-80.
- 1549 98. Maiti, T.K., P. Dixit, J. Singh, N. Talapatra, M. Ray, and S. Chattopadhyay, *A novel*
 1550 *strategy toward the advancement of proton exchange membranes through the*
 1551 *incorporation of propylsulfonic acid-functionalized graphene oxide in crosslinked acid-*
 1552 *base polymer blends*. International Journal of Hydrogen Energy, 2023. **48**(4): p. 1482-
 1553 1500.
- 1554 99. Martina, P., R. Gayathri, M.R. Pugalenthi, G. Cao, C. Liu, and M.R. Prabhu,
 1555 *Nanosulfonated silica incorporated SPEEK/SPVdF-HFP polymer blend membrane for*
 1556 *PEM fuel cell application*. Ionics, 2020. **26**: p. 3447-3458.



- 1557 100. Meng, X., C. Li, J. Wen, H. Ye, C. Cong, Q. Zhou, and L. Xu, *The effect of*
1558 *amino-modified mesoporous silica nanospheres on properties of SPEEK/HPW@*
1559 *Mesoporous Silica Nanoparticles proton exchange membrane*. Journal of the Chinese
1560 Chemical Society, 2021. **68**(7): p. 1197-1204.
- 1561 101. Sahin, A., *The development of Speek/Pva/Teos blend membrane for proton exchange*
1562 *membrane fuel cells*. Electrochimica Acta, 2018. **271**: p. 127-136.
- 1563 102. Kumar, V., S. GokulaKrishnan, G. Arthanareeswaran, A.F. Ismail, J. Jaafar, D.B. Das,
1564 and L.T. Yogarathinam, *Cloisite-and bentonite-based stable nanocomposite*
1565 *membranes for enhancement of direct methanol fuel cell applications*. Polymer
1566 Bulletin, 2023: p. 1-19.
- 1567 103. Gokulakrishnan, S., V. Kumar, G. Arthanareeswaran, A. Ismail, and J. Jaafar,
1568 *Thermally stable nanoclay and functionalized graphene oxide integrated SPEEK*
1569 *nanocomposite membranes for direct methanol fuel cell application*. Fuel, 2022. **329**:
1570 p. 125407.
- 1571 104. Charradi, K., Z. Ahmed, P. Aranda, and R. Chtourou, *Silica/montmorillonite*
1572 *nanoarchitectures and layered double hydroxide-SPEEK based composite*
1573 *membranes for fuel cells applications*. Applied Clay Science, 2019. **174**: p. 77-85.
- 1574 105. Selvakumar, K., S. Rajendran, and M. Ramesh Prabhu, *Influence of barium zirconate*
1575 *on SPEEK-based polymer electrolytes for PEM fuel cell applications*. Ionics, 2019. **25**:
1576 p. 2243-2253.
- 1577 106. Wang, Y., J. You, Z. Cheng, K. Jiang, L. Zhang, W. Cai, Y.-Q. Liu, and S. Li, *A*
1578 *promising Al-CeZrO₄/HPW-incorporated SPEEK composite membrane with improved*
1579 *proton conductivity and chemical stability for PEM fuel cells*. High Performance
1580 Polymers, 2021. **33**(3): p. 295-308.
- 1581 107. Gandhimathi, S., H. Krishnan, and D. Paradesi, *Development of proton-exchange*
1582 *polymer nanocomposite membranes for fuel cell applications*. Polymers and Polymer
1583 Composites, 2020. **28**(7): p. 492-501.
- 1584 108. Prathap, M., K. Poonkuzhali, M.M. Berlina, P. Hemalatha, and D. Paradesi, *Synthesis*
1585 *and characterization of sulfonated poly (ether ether ketone)/zinc cobalt oxide*
1586 *composite membranes for fuel cell applications*. High Performance Polymers, 2020.
1587 **32**(9): p. 984-991.
- 1588 109. Zhang, X., H. Ma, T. Pei, R. Zhang, and Y. Liu, *Anchoring HPW by amino-modified*
1589 *MIL-101 (Cr) to improve the properties of SPEEK in proton exchange membranes*.
1590 Journal of Applied Polymer Science, 2023: p. e53978.
- 1591 110. Huang, H., Y. Ma, Z. Jiang, and Z.-J. Jiang, *Spindle-like MOFs-derived porous carbon*
1592 *filled sulfonated poly (ether ether ketone): A high performance proton exchange*
1593 *membrane for direct methanol fuel cells*. Journal of Membrane Science, 2021. **636**: p.
1594 119585.
- 1595 111. Sun, L., S. Qu, X. Lv, L. Ding, J. Duan, and W. Wang, *Sulfonated Poly Ether Ether*
1596 *Ketone Membranes Reinforced by Metal–Organic Frameworks/Ionic Liquids*. ACS
1597 Applied Polymer Materials, 2023. **5**(12): p. 10081-10090.
- 1598 112. Aparna, M., P. Hemalatha, D. Paradesi, and D.A. Raj, *Design and development of*
1599 *copper trimesic acid anchored sPEEK/polyimide composite membranes for fuel cell*
1600 *applications*. ChemistrySelect, 2023. **8**(14): p. e202204584.
- 1601 113. Sun, H., B. Tang, and P. Wu, *Two-dimensional zeolitic imidazolate framework/carbon*
1602 *nanotube hybrid networks modified proton exchange membranes for improving*
1603 *transport properties*. ACS applied materials & interfaces, 2017. **9**(40): p. 35075-35085.
- 1604 114. Barjola, A., J.L. Reyes-Rodríguez, O. Solorza-Feria, E. Giménez, and V. Compan,
1605 *Novel SPEEK-ZIF-67 proton exchange nanocomposite membrane for PEMFC*
1606 *application at intermediate temperatures*. Industrial & Engineering Chemistry
1607 Research, 2021. **60**(25): p. 9107-9118.
- 1608 115. Taufiq Musa, M., N. Shaari, and S.K. Kamarudin, *Carbon nanotube, graphene oxide*
1609 *and montmorillonite as conductive fillers in polymer electrolyte membrane for fuel cell:*
1610 *an overview*. International Journal of Energy Research, 2021. **45**(2): p. 1309-1346.



- 1611 116. Gupta, N., S.M. Gupta, and S. Sharma, *Carbon nanotubes: Synthesis, properties and engineering applications*. Carbon Letters, 2019. **29**: p. 419-447.
- 1612
- 1613 117. Nqakala, N.C., *Construction of an enzyme-free electrochemical sensor based on Ag-Fe2O3/POM/RGO novel nanocomposite for hydrogen peroxide detection*. 2018.
- 1614
- 1615 118. Li, N., J. Liu, J.J. Liu, L.Z. Dong, S.L. Li, B.X. Dong, Y.H. Kan, and Y.Q. Lan, *Self-Assembly of a Phosphate-Centered Polyoxo-Titanium Cluster: Discovery of the Heteroatom Keggin Family*. Angewandte Chemie International Edition, 2019. **58**(48): p. 17260-17264.
- 1616
- 1617
- 1618
- 1619 119. Weinstock, I.A., R.E. Schreiber, and R. Neumann, *Dioxygen in Polyoxometalate Mediated Reactions*. Chemical reviews, 2017. **118** 5: p. 2680-2717.
- 1620
- 1621 120. Ponomareva, O., O. Matveeva, A. Nikiforov, I. Dobryakova, I. Kasyanov, A. Shkuropatov, and I. Ivanova, *Synthesis of butadiene from Formaldehyde and Propylene on Cesium Salts of Silicotungstic heteropoly Acid*. Petroleum Chemistry, 2021. **61**(8): p. 916-924.
- 1622
- 1623
- 1624
- 1625 121. Sánchez-Velandia, J.E., H.G. Baldoví, A.Y. Sidorenko, J.A. Becerra, and F. Martínez, *Synthesis of heterocycles compounds from condensation of limonene with aldehydes using heteropolyacids supported on metal oxides*. Molecular Catalysis, 2022. **528**: p. 112511.
- 1626
- 1627
- 1628
- 1629 122. Shaari, N., N.F. Raduwan, Y.N. Yusoff, N.A.M. Harun, and N.F.H.N. Zaiman, *Membrane and catalyst in direct methanol fuel cell and direct borohydride fuel cell application*, in *Renewable Energy Production and Distribution Volume 2*. 2023, Elsevier. p. 409-458.
- 1630
- 1631
- 1632
- 1633 123. Mao, H., X. Li, F. Xu, Z. Xiao, W. Zhang, and T. Meng, *Vapour-phase selective O-methylation of catechol with methanol over metal phosphate catalysts*. Catalysts, 2021. **11**(5): p. 531.
- 1634
- 1635
- 1636 124. Ryu, G.Y., H. Jae, K.J. Kim, H. Kim, S. Lee, Y. Jeon, D. Roh, and W.S. Chi, *Hollow Heteropoly Acid-Functionalized ZIF Composite Membrane for Proton Exchange Membrane Fuel Cells*. ACS Applied Energy Materials, 2023. **6**(8): p. 4283-4296.
- 1637
- 1638
- 1639 125. Zhang, Y., H. Zhang, C. Bi, and X. Zhu, *An inorganic/organic self-humidifying composite membranes for proton exchange membrane fuel cell application*. Electrochimica Acta, 2008. **53**(12): p. 4096-4103.
- 1640
- 1641
- 1642 126. Ghosh, A., *Synthesis of Graphene: Theory and Application*, in *Constraint Decision-Making Systems in Engineering*. 2023, IGI Global. p. 219-238.
- 1643
- 1644 127. Esrafil Dizaji, L., *Synthesis of new nano metal-organic frameworks with urea and thiourea ligands and investigation of their application in sensing, catalysis and removal of hazardous materials*. 2022, University of Antwerp.
- 1645
- 1646
- 1647 128. Collomb, D., P. Li, and S. Bending, *Frontiers of graphene-based Hall-effect sensors*. Journal of Physics: Condensed Matter, 2021. **33**(24): p. 243002.
- 1648
- 1649 129. Guo, W., M. Zhang, Z. Xue, P.K. Chu, Y. Mei, Z. Tian, and Z. Di, *Extremely High Intrinsic Carrier Mobility and Quantum Hall Effect Of Single Crystalline Graphene Grown on Ge (110)*. Advanced Materials Interfaces, 2023. **10**(23): p. 2300482.
- 1650
- 1651
- 1652 130. Mbayachi, V.B., E. Ndayiragije, T. Sammani, S. Taj, and E.R. Mbuta, *Graphene synthesis, characterization and its applications: A review*. Results in Chemistry, 2021. **3**: p. 100163.
- 1653
- 1654
- 1655 131. Das, P., B. Mandal, and S. Gumma, *L-tyrosine grafted palladium graphite oxide and sulfonated poly (ether ether ketone) based novel composite membrane for direct methanol fuel cell*. Chemical Engineering Journal, 2021. **423**: p. 130235.
- 1656
- 1657
- 1658 132. Sun, J., D. Han, M.M. Mohideen, S. Li, C. Wang, P. Hu, and Y. Liu, *Constructing vertical proton transport channels in proton exchange membranes of fuel cells*. International Journal of Hydrogen Energy, 2023.
- 1659
- 1660
- 1661 133. Guo, Z., J. Chen, J.J. Byun, R. Cai, M. Perez-Page, M. Sahoo, Z. Ji, S.J. Haigh, and S.M. Holmes, *High-performance polymer electrolyte membranes incorporated with 2D silica nanosheets in high-temperature proton exchange membrane fuel cells*. Journal of Energy Chemistry, 2022. **64**: p. 323-334.
- 1662
- 1663
- 1664



- 1665 134. Porozhnyy, M., S. Shkirskaia, D.Y. Butylskii, V. Dotsenko, E.Y. Safronova, A. Yaroslavl'tsev, S. Deabate, P. Huguet, and V. Nikonenko, *Physicochemical and electrochemical characterization of Nafion-type membranes with embedded silica nanoparticles: Effect of functionalization*. *Electrochimica Acta*, 2021. **370**: p. 137689.
- 1666
- 1667
- 1668
- 1669 135. Mohamednour, A.E.E., N.A.H.M. Nordin, M.R. Bilad, S.N.A. Shafie, S.M. Hizam, and N.I.M. Nawi, *Quantifying the impact of silica hydrophilicity and loading on membrane surface properties through response surface methodology*. *Journal of Materials Science*, 2023. **58**(35): p. 13974-13993.
- 1670
- 1671
- 1672
- 1673 136. Pal, N. and M. Agarwal, *Advances in materials process and separation mechanism of the membrane towards hydrogen separation*. *International Journal of Hydrogen Energy*, 2021. **46**(53): p. 27062-27087.
- 1674
- 1675
- 1676 137. Mohapi, M., J.S. Sefadi, M.J. Mochane, S.I. Magagula, and K. Lebelo, *Effect of LDHs and other clays on polymer composite in adsorptive removal of contaminants: a review*. *Crystals*, 2020. **10**(11): p. 957.
- 1677
- 1678
- 1679 138. Morariu, S. and M. Teodorescu, *Laponite®—A versatile component in hybrid materials for biomedical applications*. *Mem Sci Sect Romanian Acad*, 2020. **43**: p. 141-155.
- 1680
- 1681 139. Dor, M., Y. Levi-Kalishman, R.J. Day-Stirrat, Y. Mishael, and S. Emmanuel, *Assembly of clay mineral platelets, tactoids, and aggregates: Effect of mineral structure and solution salinity*. *Journal of colloid and interface science*, 2020. **566**: p. 163-170.
- 1682
- 1683
- 1684 140. Shaari, N. and S.K. Kamarudin, *Recent advances in additive-enhanced polymer electrolyte membrane properties in fuel cell applications: An overview*. *International Journal of Energy Research*, 2019. **43**(7): p. 2756-2794.
- 1685
- 1686
- 1687 141. He, S., H. Jia, Y. Lin, H. Qian, and J. Lin, *Effect of clay modification on the structure and properties of sulfonated poly (ether ether ketone)/clay nanocomposites*. *Polymer Composites*, 2016. **37**(9): p. 2632-2638.
- 1688
- 1689
- 1690 142. Chen, M., C. Zhao, F. Sun, J. Fan, H. Li, and H. Wang, *Research progress of catalyst layer and interlayer interface structures in membrane electrode assembly (MEA) for proton exchange membrane fuel cell (PEMFC) system*. *ETransportation*, 2020. **5**: p. 100075.
- 1691
- 1692
- 1693
- 1694 143. Abyzov, A., *Aluminum oxide and alumina ceramics (review). Part 1. Properties of Al₂O₃ and commercial production of dispersed Al₂O₃*. *Refractories and industrial ceramics*, 2019. **60**: p. 24-32.
- 1695
- 1696
- 1697 144. Liu, F., P. Dong, W. Lu, and K. Sun, *On formation of Al-O-C bonds at aluminum/polyamide joint interface*. *Applied Surface Science*, 2019. **466**: p. 202-209.
- 1698
- 1699 145. Kamal, A., M. Ashmawy, A.M. Algazzar, and A.H. Elsheikh, *Fabrication techniques of polymeric nanocomposites: A comprehensive review*. *Proceedings of the Institution of Mechanical Engineers, Part C: Journal of Mechanical Engineering Science*, 2022. **236**(9): p. 4843-4861.
- 1700
- 1701
- 1702
- 1703 146. Unnikrishnan, V., O. Zabihi, M. Ahmadi, Q. Li, P. Blanchard, A. Kiziltas, and M. Naebe, *Metal-organic framework structure-property relationships for high-performance multifunctional polymer nanocomposite applications*. *Journal of Materials Chemistry A*, 2021. **9**(8): p. 4348-4378.
- 1704
- 1705
- 1706
- 1707 147. Yang, S., V.V. Karve, A. Justin, I. Kochetygov, J. Espin, M. Asgari, O. Trukhina, D.T. Sun, L. Peng, and W.L. Queen, *Enhancing MOF performance through the introduction of polymer guests*. *Coordination Chemistry Reviews*, 2021. **427**: p. 213525.
- 1708
- 1709
- 1710 148. Nabipour, H., X. Wang, L. Song, and Y. Hu, *Metal-organic frameworks for flame retardant polymers application: A critical review*. *Composites Part A: Applied Science and Manufacturing*, 2020. **139**: p. 106113.
- 1711
- 1712
- 1713 149. Zheng, Z., Z. Rong, H.L. Nguyen, and O.M. Yaghi, *Structural Chemistry of Zeolitic Imidazolate Frameworks*. *Inorganic Chemistry*, 2023. **62**(51): p. 20861-20873.
- 1714
- 1715 150. Little, M.A. and A.I. Cooper, *The chemistry of porous organic molecular materials*. *Advanced Functional Materials*, 2020. **30**(41): p. 1909842.
- 1716
- 1717 151. Qian, Q., P.A. Asinger, M.J. Lee, G. Han, K. Mizrahi Rodriguez, S. Lin, F.M. Benedetti, A.X. Wu, W.S. Chi, and Z.P. Smith, *MOF-based membranes for gas separations*. *Chemical reviews*, 2020. **120**(16): p. 8161-8266.
- 1718
- 1719



- 1720 152. Yang, F., J. Wu, X. Zhu, T. Ge, and R. Wang, *Enhanced stability and hydrophobicity*
1721 *of LiX@ ZIF-8 composite synthesized environmental friendly for CO2 capture in highly*
1722 *humid flue gas*. Chemical Engineering Journal, 2021. **410**: p. 128322.
- 1723 153. Li, H., L. Li, R.-B. Lin, W. Zhou, Z. Zhang, S. Xiang, and B. Chen, *Porous metal-organic*
1724 *frameworks for gas storage and separation: Status and challenges*. EnergyChem,
1725 2019. **1**(1): p. 100006.
- 1726 154. Yang, J. and Y.W. Yang, *Metal-organic frameworks for biomedical applications*. Small,
1727 2020. **16**(10): p. 1906846.
- 1728 155. Li, D., H.-Q. Xu, L. Jiao, and H.-L. Jiang, *Metal-organic frameworks for catalysis: State*
1729 *of the art, challenges, and opportunities*. EnergyChem, 2019. **1**(1): p. 100005.
- 1730 156. Siva, V., A. Murugan, A. samad Shameem, S. Athimoolam, and S.A. Bahadur, *A new*
1731 *metal-organic hybrid material: Synthesis, structural, electro-optical properties and*
1732 *quantum chemical investigation*. Optical Materials, 2021. **121**: p. 111616.
- 1733

View Article Online
DOI: 10.1039/D4MA00628C



Data Availability Statement

View Article Online
DOI: 10.1039/D4MA00628C

Data sharing is not applicable to this article as no new data were created or analyzed in this study.

